Charles University

Faculty of Science

Study programme: Biology

Branch of study: Immunology

Bc. Michaela Přibíková

Characterization of T-cell clones from naïve and virtual memory compartment

Charakterizace naivních a virtuálně paměťových T lymfocytárních klonů

Diploma Thesis

Supervisor: Mgr. Ondřej Štěpánek, Ph.D.

Prague, 2019

Prohlášení:

Prohlašuji, že jsem diplomovou práci vypracovala samostatně na základě konzultací se svým školitelem a že jsem uvedla veškerou použitou literaturu. Tato práce ani její podstatná část nebyla předložena k získání jiného nebo stejného akademického titulu.

V Praze, 8. 8. 2019

Michaela Přibíková

Acknowledgements

Here I would like to express my special thanks of gratitude to my supervisor Dr. Ondřej Štěpánek for a great chance to work in his laboratory, for his support, valuable advices, and patient guidance. Further, I would like to thank to all other members of Laboratory of Adaptive Immunity who provided me with their advices and pleasant work environment. My acknowledgement also belongs to people from the core facilities of Institute of Molecular Genetics.

Last but not least, I would like to thank to my family, friends and boyfriend for their continuous support and encouragement during my studies.

Abstract

Virtual memory (VM) $CD8^+$ T cells represent a population of antigen-inexperienced T cells with an apparent memory phenotype. In lymphoreplete germ-free mice VM $CD8^+$ T cells represent 10-20% of all peripheral $CD8^+$ T cells. Their origin correlates with the levels of self-reactivity where the main factor that determinates the T-cell fate decision is the strength of homeostatic signals.

In the first part of this thesis, we demonstrated that VM $CD8^+$ T cells and naïve $CD8^+$ T cells had distinct TCR repertoire and T-cell subsets contained different clonotypes. Moreover, 'VM clones' were enriched among VM T cells and were also present in naïve T cells. In contrast, 'naïve clones' were almost exclusively detected in naïve T cells. Next, we characterized the signaling of particular OVA-reactive TCRs from both naïve and VM subsets. We confirmed that 6 out of 8 tested TCRs were responsive to Kb-OVA. In the last part of the thesis, we developed and optimized a qPCR-based method for the relative quantification of specific T-cell clonotypes prior to and during the immune response. This method will serve as a tool for studying the biology of particular VM and naïve T-cell subsets and their role during the immune response.

Keywords: T-cell receptor, homeostatic signaling, self-reactivity, virtual memory cells, T cells

Abstrakt

Virtuálně paměťové (VM) $CD8^+$ T buňky představují populaci tzv. antigeně-nezkušených T buněk, které mají centrálně paměťový fenotyp. Tvoří 10-20% všech periferních $CD8^+$ T buněk v neimunizované bezmikrobní myši. Formují se z vysoce autoreaktivních T buněčných klonů na periferii prostřednictvím silných homeostatických signálů T-buněčného receptoru (TCR).

V první části této diplomové práce bylo cílem porovnat TCR repertoáry VM a naivních $CD8^+$ T buněk. Ukázali jsme, že obě skupiny buněk mají tyto repertoáry odlišné a T-buněčné podmnožiny navíc obsahují odlišné klonotypy. Dále jsme zjistili, že tzv. VM klony byly přítomny jak ve VM buňkách, tak i v naivních buňkách. Na druhou stranu tzv. naivní klony se vyskytovaly pouze v buňkách naivních. V druhé části této práce bylo cílem charakterizovat signalizaci jednotlivých OVA-reaktivních TCR z VM a naivní podmnožiny T buněk. Úspěšně jsme dokázali, že šest z osmi testovaných TCR odpovídají na Kb-OVA. V poslední části práce jsme navrhli a optimalizovali qPCR metodu, která je určena pro relativní kvantifikaci specifických T-buněčných klonotypů před a během imunitní odpovědi. Tato metoda bude sloužit jako efektivní nástroj pro studování biologie jednotlivých VM a naivních podmnožin T buněk a jejich role během imunitní odpovědi.

Klíčová slova: T-buněčný receptor, homeostatická signalizace, autoreaktivita, virtuální paměťové buňky, T lymfocyty

Abbreviations

AIMT	Antigen-inexperienced memory T cells
AP-1	Activator protein 1
APC	Antigen-presenting cell
ATB	Antibiotics
B6	C57BL/6
CD	Cluster of differentiation
CD49d	Integrin alpha 4
CIP	Alkaline Phosphatase, Calf Intestinal
CM	Central memory
DAG	Diacylglycerol
DC	Dendritic cells
DDAO	Dimethyldodecylamine oxide
dNTPs	Deoxynucleotide triphosphates
DP	Double positive
EDTA	Ethylenediaminetetraacetic acid
ER	Endoplasmic reticulum
FBS	Fetal bovine serum
GF	Germ-free
GFP	Green fluorescent protein
HDAC-7	Histone deacetylase 7
IFN-γ	Interferon-gamma
IL	Interleukin
IM	Innate memory
IP_3	Inositol trisphosphate
ITAM	Immunoreceptor tyrosine-based activation motif
KO	Knock-out
LAT	Linker for activation of T cells
LB	Luria-Bertani
Lck	Lymphocyte-specific protein tyrosine kinase
LIM	Lymphopenia-induced memory

LNGFR	Low-affinity nerve growth factor receptor
Lm.OVA	Listeria monocytogenes expressing OVA
MHC	Major histocompatibility complex
MSCV	Murine Stem Cell Virus
NFAT	Nuclear factor of activated T cells
NFkB	Nuclear factor kappa-light-chain-enhancer of activated B cells
OVA	Ovalbumin
PBS	Phosphate-buffered saline
PCR	Polymerase chain reaction
PEI	Polyethylenimine
PIP_2	Phosphatidylinositol 4,5-bisphosphate
PKC	Protein kinase
PLCγ1	Phospholipase Cγ1
pMHC	Peptide major histocompatibility complex
RT	Room temperature
RT-qPCR	Real time quantitative polymerase chain reaction
SLP-76	Src homology 2 domain-containing leukocyte protein of 76 kDa
TCR	T-cell receptor
TM	True memory
Tregs	Regulatory T cells
VM	Virtual memory
WT	Wild-type
ZAP-70	Zeta chain-associated protein kinase of 70 kDa

Table of contents

1 Aims of the thesis

This thesis is part of a project studying the population of antigen-inexperienced $CD8^+$ T cells with central memory phenotype – virtual memory $CD8^+$ T cells (VM). The main aim of this thesis is to characterize some features of this novel population and analyze whether they differ in their functions compared to naïve $CD8^+$ T cells. To achieve this, the thesis is divided into three major parts:

Aim 1: Are TCR clonotypes in VM and naïve T cells different?

We hypothesized that naïve and VM T cells might have distinct TCR repertoires and that these two subsets contain different TCR clonotypes. To elucidate this question, I will compare TCRα sequences and analyze whether or not particular T-cell clones use different TCRs.

Aim 2: How particular T-cell clones response to ovalbumin (OVA) peptide? Is there any difference between 'naïve' and 'VM clones'?

Next, I will analyze the signaling of particular OVA-reactive TCRs from both naïve and VM subsets. Our hypothesis is that the intrinsic response of naïve and VM TCRs to their cognate antigen is comparable. To address this question, I will express TCRs in Jurkat cell line and characterize their response to OVA.

Aim 3: Development of qPCR-based method to study the abundance of particular T-cell clonotypes during the immune response.

The objective of this part is to develop a qPCR method which will serve to study biology of particular groups of clones. We will use this method for the analysis of the proportion of particular clones in different murine organs as well as for detection of proliferation and differences in infiltration among different organs during the immune response.

2 Introduction

2.1 T-cell development and generation of T-cell receptor

T cells are derived from hematopoietic stem cells that are found in the bone marrow. The progenitors of these cells migrate to the thymus where they undergo a series of steps to become mature T cells. The earliest developing T cells are double-negative cells (i.e., do not express either the CD4 or CD8 co-receptor) (1). T-cell receptor genes are rearranged resulting in clonal variability. This process gives rise to unique antigen-specific T-cell receptors (TCR) that have α and β chains or γ and δ chains (the majority of T cells in the thymus are αβ T cells). After successful TCRβ rearrangements, T cells become double-positive cells (i.e., start to express both CD4 and CD8 co-receptors) and start TCRα rearrangements. In this phase, T cells undergo positive selection. TCRs are tested, whether or not they are capable of binding to self-major histocompatibility complexes (MHC) I or II loaded with self-peptides. Those double-positive T cells that recognize self-peptide:self-MHC complexes are positively selected for maturation. Furthermore, T cells cease to express CD4 or CD8 to become either CD4 or CD8 positive cells. During and after double-positive stage T cells undergo negative selection (clonal deletion) and some cells are removed from the T-cell repertoire. TCRs with very high affinity for auto-reactive cells are selected and die by apoptosis or become T regulatory cells (T-regs). These processes lead to the generation of mature T cells with different range of self-reactivity (1,2).

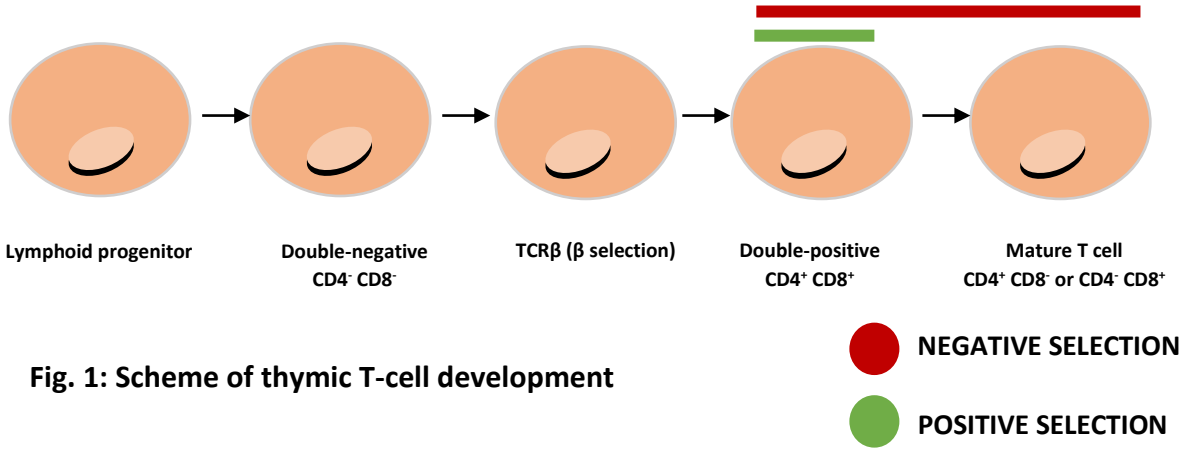

Fig. 1: Scheme of thymic T-cell development

Once T cells successfully develop in the thymus, they become antigen-inexperienced naïve T cells which re-circulate between peripheral lymphoid organs and the blood. When naïve T cells meet their cognate antigen, they start to proliferate and differentiate into antigen-experienced short-lived effector T cells, which actively defend the body against infections, and long-lived central memory (CM) T cells, which are capable of rapid response to re-infection. The main hallmark distinguishing memory T cells from naïve T cells is the expression of CD44 in mice and CD45RO in humans, which are expressed in memory, but not in naïve T cells (3,4).

2.2 T-cell receptor signaling pathway

TCR activation initiates multiple signaling pathways that are important for the determination of cell fate, cell survival, proliferation, and differentiation. At first, TCR activation leads to phosphorylation of immunoreceptor tyrosine-based activation motifs (ITAMs) of the T-cell receptor CD3 cytoplasmic components. The phosphorylated ITAMs are binding sites for a protein tyrosine kinase ZAP-70. The activation of ZAP-70 is done by lymphocyte protein kinase (Lck). Lck is recruited via its association with the co-receptors CD4 or CD8 that bind MHCII and MHCI, respectively. Once ZAP-70 becomes activated, it phosphorylates scaffold proteins LAT (i.e., linker for activation of T cells) and SLP-76 (i.e., SH2 domain containing leukocyte protein of 76kDa) (5–7).

Both LAT and SLP-76 coordinate downstream signaling events in T-cell activation and are crucial not only for T-cell activation but also for T-cell differentiation and proliferation. They recruit another key signaling molecule, phospholipase C-γ1 (PLC-γ1). Activated PLC-γ1 cleaves membrane lipid PIP_2 (phosphatidylinositol 4,5-bisphosphate) which generates two products, the second messenger inositol 1, 4, 5 - triphosphate (IP_3) and the membrane lipid diacylglycerol (DAG). The main role of IP_3 is binding to a receptor in the endoplasmic reticulum (ER) membrane and stimulation of sensitive calcium channels. Stimulation opens calcium channels to allow calcium ions (Ca_2^+) into the cytoplasm of T cells. Increase levels of Ca_2^+ in cytosol activate calcineurin-NFAT (i.e., nuclear factor of activated T cells). DAG recruits signaling protein RasGRP and protein kinase C (PKC). RasGRP is crucial for activation of Erk/MAP kinase cascade which activates the activator protein-1 (AP-1). PKC activates the transcription factor NF-κB. Collectively, NFAT, AP-1, and NF-κB initiate transcription of specific target genes that triggers differentiation and proliferation of T cells (8–11).

3 Homeostatic TCR signaling

Self-reactive T-cell clones are present in the periphery and make transient contacts with self-pMHC which are crucial for survival and expansion of peripheral naïve T cells (12–16). These interactions between self-pMHC and TCR generate so-called homeostatic signals. However, whilst these signals are required for the survival and maintenance of naïve T cells, the maintenance and longevity of memory T cells are not dependent on homeostatic signals (17–19).

As was mentioned above, TCR signaling is the main factor that triggers T-cell activation. However, TCR interactions of resting T-cell clones in the periphery with self-pMHC exhibit low-affinity. These limited signals lead to partial phosphorylation of the ITAMs in the TCR-associated ζ chain. Therefore, binding of ZAP-70 to this modified ζ chain do not trigger full T-cell activation (6,20).

Furthermore, the peripheral T-cells have a different range of self-reactivity and T cells with higher affinity to self-antigens receive more homeostatic TCR signals and outcompete T cells with a lower affinity of TCR:self-pMHC interactions (21). The strength of homeostatic TCR signals is crucial, not only for the survival of T cells but also for the generation of T-cell clones with different functional properties. Importantly, the intensity of homeostatic signals affects the fate-decision of self-reactive T cells (22,23).

3.1 The self-reactivity marker CD5

It is known, that the peripheral T-cell clones are diverse in their level of self-reactivity. The affinity between the TCR of a particular clone and self-pMHC, thus the impact of self-reactivity on the T-cell fate is difficult to analyze. However, the expression of CD5 markers is commonly used as a proxy for the level of TCR affinity for self in $CD4^+$ and $CD8^+$ T cells (21,24–26).

CD5 marker is an inhibitory surface glycoprotein which is expressed on thymocytes and all mature T cells. Its expression is tightly regulated throughout T-cell development. Levels of CD5 correlate with the intensity of positive selection and basal levels of TCR signaling (24). In the thymus, the absence of CD5 leads to enhanced signaling and activation of double-positive thymocyte which suggesting the role of CD5 as a negative regulator of the TCR signaling pathway in immature thymocytes. CD5 can negatively regulate signalling and its expression seems to be directly proportional to the TCR signal strength initially perceived (25,27–30).

Besides CD5, the second marker that may read-out levels of homeostatic signaling of T cells is a nuclear hormone factor, Nur77. To explore this, Moran et al. (31) generated transgenic mice expressing GFP from the immediate early gene Nur77 (Nur77-GFP mice). This strain is widely used for estimating the T-cell self-reactivity, because it seems to have a broader dynamic range than CD5 detection (32). However, the measurement is technically difficult compared to addressing CD5 levels. Moreover, Nur77 technique, but not CD5 technique, requires transgenic reporter mouse strain (31).

3.1.1 The role of self-reactivity in the immune response of $CD8^+$ T cells

The extent of self-reactivity is an important factor influencing the T-cell fate decisions and effector functions. The levels of self-reactivity might predict the properties of particular T-cell clones, such as the ability to respond to foreign cognate antigens (21,33).

Fulton et al. (21) examined immune properties of naïve $CD8^+$ T cells with a different level of self-reactivity. They sorted $CD44^-$ $CD5^{hi}$ (high self-reactivity) and $CD44^-$ $CD5^{lo}$ (low self-reactivity) $CD8^+$ T cells from C57Bl/6 wild type (WT) mice and compared their gene expression profiles. They observed that $CD5^{hi}$ expressed slightly higher levels of CD44, CD122, T-bet and CXCR3 which might correlate with the higher tendency of $CD5^{hi}$ T cells to differentiate into memory T cells (21).

Multiple *in vivo* experiments were performed to analyze whether $CD5^{hi}$ naïve T cells respond to foreign antigens better than $CD5^{lo}$ naïve T cells. These experiments showed enhanced ability of $CD5^{hi}$ naïve T cells to provide the immune response against the pathogen. The advantage of $CD5^{hi}$ $CD8^+$ naïve T cells consisted of more efficient initial activation and response to pathogens. Moreover, the clonal burst size of $CD5^{hi}$ T cells was greater and these cells also displayed enhanced sensitivity to inflammatory cues (21).

Another study (33) analyzed three different $CD8^+$ T-cell clones specific to *Toxoplasma gondii* Rop7 epitope presented by H-2 L^d. They analyzed activation and proliferation 9 days after infection with *Toxoplasma gondii in vivo*. Although one clone expanded less in response to *Toxoplasma gondii*, the expression of CD25, CD44 and CD62L was comparable among all three clones which suggesting that all T cells responded to the antigen. The analysis of activation upon antigenic stimulation *in vitro* showed differences in cytokine production among all three clones. Moreover, the clone that expanded less in response to *Toxoplasma gondii* had a higher tendency to trigger cell death. The analysis of protein phosphorylation upon antigenic stimulation showed TCR signaling occurs in a distinct manner in all three Rop7 CD8 T-cell clones (33,34).

Next, they analyzed whether the reduced cytokine production and proliferation of some T-cell clones correlated with differences in homeostatic signaling. The strength of homeostatic signals, thence the self-reactivity was analyzed based on the expression of CD5 and Nur77-GFP in Nur77-GFP transgenic mice (31). In this experiment, they observed lower expression of CD5 and Nur77-GFP by the clone which showed reduced cytokine production and proliferation. These data indicated the correlation between reduced cytokine production and proliferation and decreased self-reactivity. On the other hand, the $CD5^{hi}$ T-cell clone with the strongest ability to proliferate upon infection had the highest affinity for self-antigens (33).

Collectively, these studies (21,33) showed the correlation between the self-reactivity and effector functions of $CD8^{+}$ T cells and their recruitment into the foreign-pMHC specific response. Consequently, the T-cell clones with higher self-reactivity display enhanced a superior initial response and effector functions.

3.1.2 The role of self-reactivity in primary and secondary responses of $CD4^+$ T cells

Similarly to $CD8^+$ T-cells, the self-reactivity may determine the functional properties of $CD4^+$ T cells as well (35–37).

Two $CD4^+$ T-cell clones with the identical affinity for the cognate antigen were tested during different stages of the immune response. Primary response was measured 7 days after infection, whereas secondary response was measured 39 days after infection. These clones recognized an epitope of amino acids 190–205 of the *Listeria monocytogenes* (Lm) virulence factor listeriolysin O (LLO) (35,37). The difference in the self-reactivity between these two clones was analyzed based on the expression of CD5 (24,25). It was observed, that the less self-reactive ($CD5^{lo}$) $CD4^+$ T-cell clone was more efficient during the primary response to *Listeria monocytogenes* infection than more self-reactive ($CD5^{hi}$) $CD4^+$ T-cell clone. After infection, the $CD5^{lo}$ clone have dramatic TCR down-regulation which prevented an effective $CD4^+$ secondary response. On the other hand, the $CD5^{hi}$ $CD4^+$ T-cell clone had a more efficient secondary response to the same infection (35).

These experiments suggest that a relatively highly self-reactive CD4 T cells showed more robust initial response compared to clones with lower self-reactivity. However, this stronger reactivity of the highly self-reactive T cells made them more susceptible to IL-2 driven cell death which caused the limited expansion of these T cells during the primary immune response (35,37).

3.2 Homeostatic signals in survival and tolerance of $CD4^+$ and $CD8^+$ T cells

Homeostatic signals are important for T-cells homeostasis and maintenance. Their loss leads to a reduction in T-cells numbers. However, the reduction of homeostatic signals does not affect the persistence of both $CD8^+$ and $CD4^+$ memory T cells (17–19).

Some studies (38–41) examined the impact of TCR ablation and important signaling molecules to the survival and maintenance of T cells.

Polic et al. (38) did inducible deletion of the TCR by treating $C\alpha^{fl/fl}$ Mx-Cre (Cre-Lox system) mice with poly(I):poly(C) (pI:C). They compared TCR^+ and TCR^- T cells over time. They showed that the percentage of TCR^- $CD8^+$ naïve T cells, but not TCR^+ $CD8^+$ naïve T cells, rapidly declined. On the other hand, the percentage of TCR^- $CD8^+$ memory T cells declined slowly, whilst TCR^+ $CD8^+$ memory T cells increased over time. TCR^- $CD4^+$ naïve T cells declined much slower compare to TCR^- $CD8^+$ naïve T cells. Furthermore, the comparison of $CD4^+$ memory T cells showed that TCR^- $CD4^+$ cells persisted at constant levels, whilst the percentage of TCR^+ $CD4^+$ T cells strongly increased over time (38).

Recent study (39) examined the role of homeostatic TCR signals in the absence of a key signaling molecule, SLP-76 during the contraction and maintenance of immune response. The tamoxifen-induced deletion of SLP-76 caused a substantial decrease of naïve $CD8^+$ $CD44^-$ T cells (13,39). However, analysis of antigen-specific memory $CD8^+$ $CD44^+$ T cells in the absence of SLP-76 didn't show decreased numbers of cells 48 weeks after infection. Moreover, the long-term absence of SLP-76 didn't affect the expression of surface TCR and markers of T-cell memory (39).

A similar observation was made using $CD4^+$ T cells. SLP-76 is crucial for antigen-specific $CD4^+$ memory T-cells and their response to antigenic TCR signaling. However, the persistence of these cells is not affected in the absence of SLP-76 (42).

Another recent work (40) studied the role of homeostatic signals in the absence of trans-membrane adapter LAT. It is known that activated $CD4^+$ T cells differentiate into distinct subsets of effector T cells (i.e., Th1, Th2, Th17 and/or Tfh) that produce specific cytokines. Th1 cells produce IFN-γ and IL-2 while Th2 express IL-4, IL-5, or IL-13. Third major cell type that designed Th17 cells has been characterized by expression of IL-17A, IL-17F, and IL-22 that are not produced by either Th1 or Th2 cells. These cytokines, together with TCR signals and transcriptions factors (i.e., T-bet, GATA-3, Rorγt, and FoxP3) are crucial for the polarization of $CD4^+$ T cells (43–45). However, some $CD4^+$ T cells remain in resting, naïve state and it is still unclear how these cells avoid mechanisms of spontaneous Th cell differentiation. Nonetheless, Myers et al (40) showed that the homeostatic signals through LAT are important for the maintenance of undifferentiated state of naïve $CD4^+$ T cells (40).

The homeostatic signals through LAT constitutively phosphorylate transcriptional factor HDAC7 (i.e., Histone deacetylase 7) and its export from the nucleus. This process promotes the expression of immune-modulatory genes Nur77 and Irf4 (40,46,47). Moreover, it was showed that Nur77 and Irf4 are important factors that regulate proliferation of naïve $CD4^+$ T cells and their polarization. Nur77 and Irf4 are important regulators for maintaining the naïve, undifferentiated state.

In addition, the homeostatic signals in $CD4^+$ T cells thus self-recognition are important for either suppressive responses that weakening (48,49) or improving foreign antigen sensitivity of TCR (50). It was showed that TCR ablation in Tregs did not affect the expression of a signature transcriptional factor FoxP3. However, the expression of Nur77 and Irf4 was significantly reduced. Thence, homeostatic signals through LAT-HDAC7 may also regulate the homeostasis of Tregs (41,51).

In summary, inducible TCR ablation revealed the role of homeostatic TCR signaling for the maintenance and function of T cells. $CD8^+$ and $CD4^+$ TCR-deficient naïve T cells decay over time, whereas TCR-deficient memory T-cells decline very slowly (CD8) or not at all (CD4) (38).

4 Antigen-inexperienced memory CD8$^+$ T cells

In the last few years, a population of CD8$^+$ T cells with apparent memory phenotype has been described. These so-called antigen-inexperienced memory T cells (AIMT cells) represent 10-20% of all CD8$^+$ T cells in young mice (reviewed in 52). AIMT cells can be divided into three major groups: I. Innate memory (IM) T cells that are formed in the thymus (53,54), II. Lymphopenia-induced memory (LIM) T cells that are formed in the periphery via homeostatic proliferation during lymphopenia (55), III. Virtual memory (VM) T cells that are formed in the periphery in wild type (WT) unimmunized mice. (56,57).

4.1 AIMT cells and the role of cytokines in their formation

The nomenclature of AIMT cells is still not fully established. In this chapter, I will briefly summarize the importance of various interleukins in the generation of particular AIMT-cell populations to better understand the nomenclature of AIMT cells. The main difference between IM, LIM, and VM T cells is the role of different cytokines in their development. Interleukin 4 (IL-4) is crucial for the formation of IM CD8$^+$ T cells (58). LIM and VM T cells are formed in the periphery of C57Bl/6 mice and their generation depends largely on IL-7 (59) and IL-15 and minimally on IL-4 (60) (Fig.2).

The strain-dependent importance of specific cytokine in AIMT cell formation was confirmed by Tripathi et al. (61) who compared the presence of AIMT CD8$^+$ T cells in both IL-4 and/or IL-15 deficient Balb/c and C57Bl/6 mice. They observed that formation of VM CD8$^+$ T cells in Balb/c mice largely depends on IL-4 and partially on IL-15, whereas it is vice versa in C57Bl/6 mice. Tripathi et al. (61) showed that dependency on different cytokines is mouse strain specific. Some studies (61,62) described IL-4 dependent population of AIMT cells in the periphery of Balb/c mice. However, the difference between peripherally-induced IL-4 and IL-15 VM CD8$^+$ T cells and thymic-induced IL-4 innate memory T cells is still poorly understood.

Another study (63) showed, that increased levels of IL-4 in Ndfip1 (i.e., adaptor protein) deficient C57Bl/6 mice lead to the generation of peripheral AIMT CD8$^+$ T cells. The similar observation was made using ITK (the Tec family nonreceptor tyrosine kinase) deficient C57Bl/6 mice (64,65). Their data suggest that the genetically elevated production of IL-4 leads to the generation of small part of AIMT CD8$^+$ T cells in C57Bl/6 mice in the thymus (63–65).

In summary, IL-4, IL-7, and IL-15 are major cytokines crucial for the formation of AIMT cells.

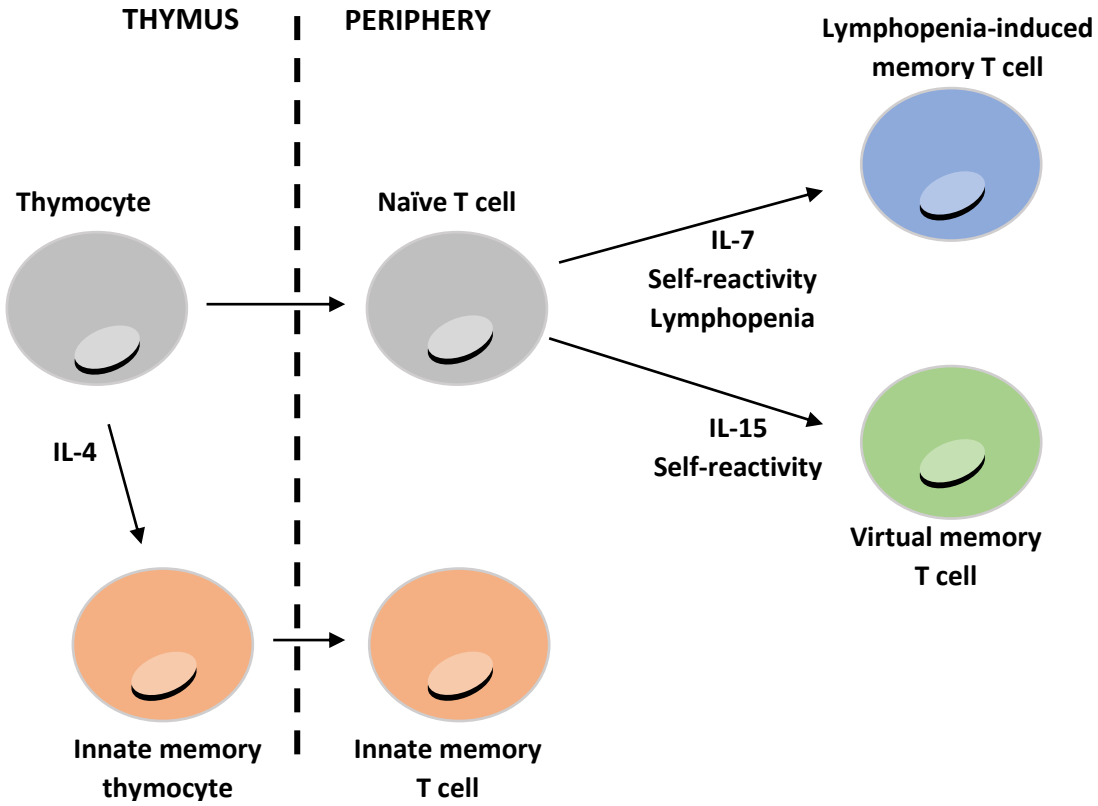

Fig.2: Origin of AIMT cells – formation of IM, LIM and VM T cells in the thymus and in the periphery under the control of IL-4, IL-7, and IL-15 (modified from 66).

4.2 The relationship between LIM and VM CD8$^+$ T cells

LIM CD8$^+$ T cells are generated during experimentally induced lymphopenia. Their abilities to provide rapid immune protection most likely by up-regulation of interferon gamma (IFN-γ) are similar to true memory (TM) T cells. However, they don't represent true immunological memory (55).

Based on detail analysis of gene expression profiles, immune responses, and role of TCRs in the formation of LIM CD8$^+$ T and VM CD8$^+$ T cells, we concluded that these two populations most likely represent the identical cell type (reviewed in 66), whilst IM CD8$^+$ T cells might represent a different population with distinct functional features.

The main objective of this thesis are VM CD8$^+$ T cells, therefore in the next chapter I will describe important features of VM CD8$^+$ T cells in more detail.

4.3 Virtual memory CD8$^+$ T cells

As mentioned above, antigen-specific T cells with central memory phenotype without prior antigenic exposure were observed in the periphery of healthy unimmunized lymphoreplete WT mice. Since the generation of these T cells is independent of infection or immunization, they were termed virtual memory CD8$^+$ T cells (56).

VM CD8$^+$ T cells appear soon after birth in normal mice, as well as in germ-free (GF) mice, thence they could be formed by homeostatic mechanisms in newborn lymphopenic mice where the first T cells emigrating from the thymus differentiate into VM CD8$^+$ T cells. In addition, they accumulate during ageing and therefore they could be also formed during age-related lymphopenia. However, most likely they differentiate from highly self-reactive T-cell clones that receive strong TCR signals in the periphery (56,57,62,67,68).

4.3.1 Phenotypic markers of VM CD8$^+$ T cells and their importance in the development

VM CD8$^+$ T cells express multiple phenotypic markers of TM T cells, such as CD44, CD62L (i.e., L selectin), and Ly6C. So far, the only marker distinguishing VM CD8$^+$ T cells and TM T cells is the lower expression of α4-integrin (CD49d) in VM CD8$^+$ T cells (56,69).

To better understand the gene expression profiles and differences between VM CD8$^+$ T cells, TM T cells, and naïve T cells, we (70) and others (57) used deep RNA sequencing method. We found many genes that are differently expressed in VM CD8$^+$ T cells compared to naïve and TM T cells. This analysis of gene expression profiles suggests that VM CD8$^+$ T cells represent an intermediate stage between naïve and true memory T cells. Moreover, we analyzed two genes (CX3CR1 and NRP1) that were expressed significantly differently in VM CD8$^+$ T cells and TM T cells on the protein level. It was observed that a subset of TM T cells but not VM CD8$^+$ T cell expressed these markers. Hence, the lower expression of CXC3CR1 and NRP1 can be another marker distinguishing TM T cells from VM CD8$^+$ T cells (70).

4.3.2 Protective abilities of VM CD8$^+$ T cells

One hallmark suggesting that VM CD8$^+$ T cells could provide better protection against infection than naïve T cells is a rapid production of IFN-γ after TCR stimulation (56). It was showed, that this expression is higher compared to naïve T cells, but slightly lower in comparison with TM T cells (69). Therefore VM CD8$^+$ T cells may be able to participate in initial immune responses (56).

Some studies (60,69) examined immune responses of VM and naïve cells against virulent Lm *in vivo*. VM CD8$^+$ T cells were more efficient than naïve T cells in providing protection and thus can provide potent antigen-specific protective immunity against Lm on a per cell basis (60,69).

Moreover, novel studies (71,72) showed that infection caused by parasitic helminths resulted in the expansion of VM CD8$^+$ T cells that can provide broad protection against bacterial/viral infection.

4.3.3 Role of TCR and self-reactivity in the development of VM CD8$^+$ T cells

As mentioned, one possible explanation of how VM CD8$^+$ T cells are generated is through strong homeostatic TCR signals. Renkema et al. (62) tried to analyze whether the TCR specificity is important for VM CD8$^+$ T-cells formation. Their analysis of TCR transgenic OT-I Rag$^+$ population showed an accumulation of VM CD8$^+$ T cells in old mice. Moreover, they observed that age-related conversion of VM CD8$^+$ T cells depends on the secondary TCR rearrangements in OT-I Rag$^+$ mice, but not in Rag KO mice that cannot recombine the endogenous TCRs. They proposed that VM CD8$^+$ T cells are formed from clones using endogenous TCRα and thus TCR specificity plays role in the VM CD8$^+$ T cells formation during ageing, but not during the neonatal period (62).

White et al. (57) observed that VM CD8$^+$ T cells development correlates with the expression of a self-reactivity marker, CD5. Their data suggested that VM CD8$^+$ T cells are preferentially derived from naïve T cells with relatively high levels of self-reactivity. However, they did not analyze the fate of individual T-cell clones in VM CD8$^+$ T cells formation (57).

The observation made by White et al. (57) that CD5^{hi} naïve T cells have higher tendency to convert into VM T cells leads us to the hypothesis that the formation of VM T cells is a so far unappreciated T-cell fate decision check point, where the intensity of homeostatic TCR signals is the critical decisive factor.

5 Methods

5.1 Aim 1: TCRα sequencing

5.1.1 RNA isolation

$CD44^{lo}$ and $CD44^{hi}$ $CD8^{+}$ memory T cells from GF Vβ5 mice were sorted and RNA was isolated using Trizol reagent (ThermoFisher Scientific) and RNA clean & concentrator kit (Zymoresearch, R1013) (Done by Dr. Ondřej Štěpánek).

5.1.2 cDNA transcription and amplification

5 – 10 µl of RNA (total RNA - 1 or 2 µg) were mixed with 1 µl of TRAC EcoRI primer and water to final volume 12.5 µl. The samples were incubated at 65°C for 5 minutes, then put on ice for 5 minutes and briefly vortexed. 5X Reaction Buffer, dNTPs, Ribolock RNase inhibitor, RevertAid reverse transcriptase were added to the samples (Table 1), briefly centrifuged and incubated at 42°C for 1 hour. The reaction was terminated by incubation at 70°C for 10 minutes. (All reagents were provided by ThermoFisher Scientific.)

REAGENTS	Con.	VOLUME
5X Reaction buffer		4 µl
Ribolock RNase inhibitor	20 U	0.5 µl
RevertAid reverse transcriptase	200 U	1 µl
dNTPs	10 mM	2 µl
previously prepared RNA+TRAC EcoRI primer		12.5 µl
Final volume		**20 µl**

Table 1: Preparation of Reverse transcription

Obtained cDNA was diluted 25x and amplified by PCR using Phusion polymerase (New England Biolabs) and following primers:

1. TRACrev (EcoRI) 5'-TCAGACgaattcTCAACTGGACCACAGCCTCA
2. TRAV14for (XhoI) 5'- GTAGCTctcgagATGGACAAGATCCTGACAGCA
3. TRAV12for (XhoI) 5'- GTAGCTctcgagATGCGTCCTGDCACCTGCTC

The following reagents were mixed as in table 2:

REAGENTS	VOLUME
Template DNA	3 µl
F primer (10 µM)	1.5 µl
R primer (10 µM)	1.5 µl
dNTPs (10 mM)	1 µl
5x HF buffer	10 µl
Phusion polymerase	0.5 µl
Water	32.5 µl
Final volume	**50 µl**

Table 2: PCR reaction

The reaction setup for PCR reaction was as in the following table 3:

	STEP	TEMPERATURE	TIME
1.	Initial denaturation	98°C	30 s
2.	Denaturation	98°C	5 s
3.	Annealing	68°C	20 s
4.	Elongation	72°C	30 s
	Cycle to step 2 – 40x		
5.	Final Extension	72°C	5 min
6.	Final hold	4°C	Hold

Table 3: Phusion PCR setup

The concentration of obtained DNA product was measured on NanoDrop spectrophotometer (ThermoFisher).

5.1.3 Preparation of cDNA construct

PCR products were separated using horizontal electrophoresis on 1% agarose gel in TAE buffer. Desired fragments were isolated from gel and purified using the Zymoclean Gel DNA Recovery Kit (Zymo Research). Purified PCR products and pBluescript plasmid were prepared for cleavage reaction using specific restriction enzymes (1 µl of XhoI, 1 µl of EcoRI and 2 µl of 10x Cutsmart buffer). Samples were digested at 37°C for 3 hours. 2 µl of Alkaline Phosphatase (CIP; nonspecifically catalyzes the dephosphorylation of 5´ and 3´ ends of DNA and RNA phosphomonoesters) (New England Biolabs) were added to samples 30 minutes before the end of digestion.

Samples were incubated at 80°C for 10 minutes to inhibit the reaction. Digested samples were separated on 1% agarose gel in TAE buffer, fragments were isolated from gel and cDNA was purified using Zymoclean Gel DNA Recovery Kit (Zymo Research). The concentration of obtained cDNA inserts and pBluescript vector were measured on NanoDrop spectrophotometer (ThermoFisher Scientific).

The amount of cut insert and vector was determined and insert was mixed with vector in molar ration 4:1. Ligation reaction was performed by the T4 DNA ligase enzyme (New England Biolabs). The mixture obtained: vector DNA, insert DNA, Ligase buffer, T4 DNA ligase enzyme and water. Samples were incubated at 16°C overnight. The ligation reaction was inhibited by putting samples at 65°C for 10 minutes, then briefly centrifuged and put on ice for 5 minutes.

5.1.4 Transformation

80 µl of competent bacteria *Escherichia Coli* were added to sample mixture, incubated on ice for 30 minutes and then transformed by incubation at 42°C for 1 minute. 300 µl of sterile Luria-Bertani (LB) media were added and samples were shaken at 37°C for 30 minutes. Bacteria were spread with sterile hockey on ampicillin-containing LB agar plates and incubated at 37°C overnight. Next day, several colonies were picked with a tip and inoculated into 1.5 ml of LB media with ATB and incubated on shaker overnight.

5.1.5 Clone sequencing

1 ml of bacterial culture was transferred into Eppendorf and centrifuged (5 minutes, 13000g). The pellets were re-suspended in 100 µl of solution I (Table 4) and mixed properly. 200 µl of solution II (Table 4) were added to the samples, mixed and incubated at room temperature (RT) for 10 minutes. Then 150 µl of solution III (Table 4) were added and samples were centrifuged (5 minutes, 13000g). Supernatant was transferred into a clean tube and mixed with 1 ml of 100% ethanol and incubated at -20°C for 20 minutes. After 20 minutes samples were centrifuged (5 minutes, 13000g) and pellets were re-suspended with 70% ethanol, centrifuged (5 minutes, 13000g). Pellets were air-dried and re-suspended in 25 µl of water.

Solution I	50 mM Glucose, 25 mM Tris-Cl, 10 mM EDTA, pH 8
Solution II	0.2 M NaOH, 1% SDS
Solution III	3 M potassium acetate, 2 M acetic acid

Table 4: Chemicals used in DNA plasmid isolation

Samples were prepared for restriction analysis using specific restriction enzymes (0.2 µl of XhoI, 0.2 µl of EcoRI and 1 µl of 10x Cutsmart buffer). Incubated at 37°C for 2 hours and run on 1% agarose gel in TAE buffer. Samples with the strongest bend were sequenced by Sanger sequencing (GATC Biotech) using T7 primer.

1. T7 primer 5'- TAATACGACTCACTATAGGG

Sanger sequences were analyzed using SeqMan Pro and GraphPad Prism 5 software.

Some experiments and analysis were done with the help of Dr. Martina Huranová.

5.2 Aim 2: Characterization of particular TCRs

5.2.1 Viruses preparation from MSCV plasmids

Selected clones were cloned into pMSCV-ires-GFP and pMSCV-ires-LNGFR (both vectors were kindly provided by the lab of Dr. Tomáš Brdička) via EcoRI and XhoI enzymes (New England Biolab) and used for transfection with polyethylenimine (PEI). Cloning to pMSCV-ires-LNGFR was done by Dr. Aleš Drobek.

Phoenix AMPHO cells were thawed and cultured in Petri dish with 10 ml of DMEM (Sigma Aldrich) media with antibiotics (ATB) and 10% fetal bovine serum FBS (Gibco). On day 1, when the cells reached 70 – 80% confluence, the medium in the Petri dishes was changed for ATB free media without serum. 1 ml of ATB free DMEM with 0.5% serum in the microtube was mixed with 30 µg of DNA and 75 µl of PEI (con: 1 µg/µl) and incubated at 37°C for 10 minutes. Then the mixture of DNA and PEI was added to the cells in Petri dishes and incubated at 37°C for 3 hours. Then the medium was replaced with fresh DMEM with 10% serum and no ATB. On day 2, the medium in the Petri dishes was changed for production medium. On day 4, the cells from Petri dishes were centrifuged (5 minutes, 500g) and the supernatant was transferred into microtubes and stored at -80°C.

5.2.2 Spinfection of Jurkat cell line

$1x10^6$ of Jurkat T cells with TCRβ and human CD8 were re-suspended in 2 ml of viral supernatant. We used two different Jurkat cell lines (i.e., Jurkat $CD8^+$ OT-I TCRβ and LckKO $CD8^+$ OT-I TCRβ reintroduced with Lck containing FLAG tag). 8 µg/µl of polybrene were added to the samples and centrifuged (45 minutes, 2500rpm, 30°C). Cells were incubated at 37°C overnight. On day 2, cells were transferred into a 15 ml falcon tube, centrifuged (10 minutes, 400g) and re-suspended in fresh RPMI medium with ATB and 10% serum. On day 4, cells were transferred from six-well plate to the tissue culture flasks and let to grow. When the cells were grown, GFP positive and LNGFR (stained for Vα2 in PE (BioLegend)) positive cells were sorted on the BD Influx Cell Sorter (BD Biosciences) in the core facility.

5.2.3 Antigen Presentation Assay

Required amount of T2Kb cells ($2x10^5$ per sample) was re-suspended in RPMI medium (Sigma Aldrich), stained with DDAO dye (ThermoFisher Scientific), diluted 1500x and incubated at 37°C for 10 minutes. Then cells were washed in RPMI medium, centrifuged (5 minutes, 500g). $2x10^5$ of T2Kb cells were re-suspended in 100 µl RPMI media with OVA peptide (SIINFEKL, storage concentration 2mM, Eurogentec) and incubated at 37°C for 2 hours. T2Kb cells were loaded with different concentration of OVA. Concentration series were made by putting 200 µl of RPMI media with 2 µl of OVA in first well without T2Kb cells. 20 µl from the first well were added to the second well with 180 µl of RPMI media and mixed. 20 µl from the second well were added to the third well with 180 µl of RPMI media and mixed etc. Then T2Kb cells were re-suspended with 100 µl of RPMI with OVA in different concentration.

First well contained unstained sample as a control, second well contained Jurkat cell clone without T2Kb cells, third well contained Jurkat cell clone with T2Kb cells without OVA, following wells contained OVA-loaded T2Kb cells with Jurkat cell clone (concentration series: $1 \times 10^{-5} – 1 \times 10^{-12}$) (Table 5).

After 2 hours T2Kb cells were centrifuged (5 minutes, 500g) and mixed with $2x10^5$ of particular Jurkat cell clone in 100 µl. 100 µl of fresh RPMI were added to the mixture and incubate at 37°C overnight. Cells were incubated in the flat-bottom 96-well tissue culture plate in total volume of 200 µl. The next day, the plate with the cells were centrifuged (5 minutes, 500g), then the cells were re-suspended in FACS buffer (PBS, 2% FBS, 1mM EDTA, 0,1% NaN_3), stained with α-huCD69-PE-Cy7 (BioLegend) and incubated on ice for 45 minutes. Stained cells were washed twice with FACS buffer and analyzed on LSRII.

Data from DIVA Software were imported to a FlowJo for analysing flow cytometry data. Results were imported to a Microsoft Excel and analyzed using GraphPad Prism 5 software.

SAMPLE	WELL 1	WELL 2	WELL 3	WELL 4 conc. 1×10^{-5}
Jurkat Clone 1	Unstained cells	Jurkat cells Clone 1	Untreated T2Kb + Jurkat cells	OVA-loaded T2Kb + Jurkat clone 1

Table 5: organization of the samples

5.2.4 Tetramer staining

Particular Jurkat T-cell clones were re-suspended in FACS buffer and stained with H-2Kb/OVA-PE (SIIQFEHL) MHC Tetramer. Cells were stained at RT for 30 minutes, then washed twice with FACS buffer and analyzed on LSRII.

5.2.5 Cell culture

Phoenix AMPHO cells were cultivated in complete DMEM medium, Jurkat T-cell clones and T2Kb cells were cultivated in complete RPMI medium. Both media contained 10% FBS (Gibco) and antibiotics streptomycin, penicillin and gentamicin. All cells were cultured at 37°C, 5% CO_2. $5x10^6$ cells from each culture were frozen in FBS with 5% DMSO and stored in liquid nitrogen.

5.3 Aim 3: qPCR – based method

5.3.1 Primers design

For design were used sequences (VM and naïve) that were acquired in the first part of this thesis. Website Primer-BLAST was used for finding specific primers. PCR product size was 70 – 200. The selected primers used for qPCR are in table 6.

PRIMER NAME	5′ → 3′ sequence
VM1_F	AGGCCCTGCACTCCTGATA
VM1_R	TGTATGGATGAACCACGAGGC
VM2_F	AGGCCCTGCACTCCTGATA
VM2_R	TATGGATGAACCACGAGGCTG
N1_F	TTCTGGATGTTGGGCTTCACCA
N1_R	GGAGAAAAAGCTCTCCTTGCAC
N2_F	CTCTCCTTGCACATCACAGACT
N2_R	GGATGTTGGGCTTCACCACC
qTCRα_F	ACATCCAGAACCCAGAACCTG
qTCRα_R	AAAGTCGGTGAACAGGCAGA

Table 6: Primers used for qPCR

5.3.2 Experimental animals

All used mice were older than 5 months and had C57Bl/6j background. Ly5.1 mice were used for isolation of dendritic cells (DCs) from bone marrow. Vβ5 mice were used for transfection with DCs or with Lm.OVA. C57Bl/6j and OT-I mice were used as a negative and positive control for tetramer testing. Both males and females were used for experiments. They were housed in specific pathogen-free conditions in the facility of Institute of Molecular Genetics of the ASCR, v.v.i.

5.3.3 Dendritic cells preparation

DCs were isolated from the back legs of Ly5.1 mice. Legs were cut above the hip joint in order to access the femur and tibia. The bones were debrided from the muscles and tissue, washed in ethanol and put to the Petri dish with 2 ml of PBS 1x (8 g/l NaCl, 0.2 g/l KCl, 0.2 g/l KH2PO4, 1.15 g/l Na2HPO4) and kept on ice. Next, the bones were cut on both ends. Bone marrow was flushed with 5 ml of PBS using 0.45 mm sterile syringe. Bones were flushed 3 – 4 times until the bones were completely white. The samples were centrifuged (5 minutes, 500g). The pellets were re-suspended in 1 ml of ACK (Ammonium-Chloride-Potassium) Lysis Buffer. After 1 minute 9 ml of PBS were added and cells were centrifuged (5 minutes, 500g). The pellets were re-suspended in 15 ml of complete IMDM media (10% FBS + antibiotics – streptomycin/penicillin (IMG Core Facility – Media and Glass Washing) and transferred to the non-treated Petri dishes. 200 µl of Lutz (supernatant from Lutz cells containing growth factor – GM-SCF) were added to the Petri dishes. The cells were incubated at 37°C incubator with 5% CO_2.

Every 2 – 3 days the medium was changed. The cells were transferred from Petri dishes to 15 ml falcons, centrifuged (5 minutes, 300g) and re-suspended in fresh 15 ml of complete IMDM media with 200 µl of Lutz.

5.3.4 Mice immunization with DCs

DCs were harvested on day 10. Cells were gently washed by pipetting up and down for 4 – 5 times. All medium from Petri dish was transferred to the falcon tube and centrifuged (5 minutes, 300g). The pellet was re-suspended in 1 ml of IMDM medium and added to the Petri dish with 9 ml of fresh IMDM media (total volume in one Petri dish: 10 ml). Then 1 µl of lipopolysaccharide (LPS) and 1 µl of OVA peptide were added to the cells. Cells were incubated at 37°C for 3 hours.

After three hours, 10 ml of IMDM media were transferred to a new falcon tube. To the Petri dish were added 4 – 5 ml of Ethylenediaminetetraacetic acid (EDTA – 10mM in PBS) (IMG Core Facility – Media and Glass Washing) to detach adhesive cells. After 5 minutes, cells were washed by pipetting up and down and transferred to the falcon tube with IMDM medium. Cells were briefly mixed and centrifuged (5 minutes, 300g). The pellet was re-suspended in 10 ml of PBS and counted on cell counter. 1 x 10^6 of DCs in 200 µl of PBS were intravenously injected into Vβ5 mice. The mice were analyzed 3 days after injection.

5.3.5 Mice immunization with Lm.OVA

Listeria (stored at -80°C) from stock was inoculated into 3 ml of media (Heart brain infusion broth) in a 15 ml falcon tube and let to grow on shaker for 3 hours at 37°C. Then 10 ml of PBS were added to the falcon tube with Listeria and HBI medium and centrifuge for 10 minutes on maximal speed. The pellet was re-suspended in 3 ml of PBS and optical density was measured. The Listeria was diluted to final concentration 5000 CFU in 200 µl and intravenously injected into Vβ5 mice. Mice were analyzed 3 days after injection.

5.3.6 T cells preparation for sort analysis

Spleen was isolated from Vβ5 mice, placed on Petri dish with 1 ml of PBS and mashed. Cells were filtered to a 15 ml falcon tube and centrifuged (5 minutes, 400g) and re-suspended in 1 ml of ACK Lysis Buffer. Samples were incubated for 2 minutes on RT and then mixed with 9 ml of PBS and centrifuged (5 minutes, 400g). The pellets were re-suspended in the required amount of PBS and stained with CD4-FITC (BioLegend) and B220-FITC (BioLegend) antibodies. The samples were on ice for 30 minutes, washed 2 times in PBS, re-suspended in the required amount of PBS and Anti –FITC MicroBeads (MACS Miltenyi Biotec) were added. The samples were gently mixed, incubated on ice for 30 minutes and washed with PBS. Cells were separated on fully automated cell separation – autoMACS Pro Separator using depletion program – DepleteS which removed cells with low antigen expression. Negatively selected cells were centrifuged (5 minutes, 400g) and stained for sort (Table 7).

$CD8^+$ Kb-OVA^+ cells were sorted on the BD Influx Cell Sorter (BD Biosciences) in the core facility.

		CONJUGATE	COMPANY	DILUTION
1.	CD8a	BV421	BioLegend	200x
2.	Viability	APC-Cy7	ThermoFisher Scientific	500x
3.	Kb-OVA	PE		100x

Table 7: Antibodies used for staining

5.3.7 Purifying RNA from cells

RNA was isolated using Rneasy Plus Micro Kit (Qiagen). Sorted cells were collected to an appropriate volume of Buffer RLT Plus (Qiagen) containing B-mercaptoethanol (Sigma Aldrich). The lysate was transferred to a gDNA Eliminator spin column placed in a 2 ml collection tube and centrifuged (30 seconds, 8000g). The flow-through was mixed with 70% ethanol, mixed and transferred to a Rneasy MinElute spin column placed in a 2 ml collection tube. The sample was centrifuged (30 seconds, 8000g) and flow-through was discarded. 700 µl of Buffer RW1 (Qiagen) was added to Rneasy MinElute spin column, centrifuged (30 seconds, 8000g) and flow-through was discarded. 500 µl of Buffer RPE (Qiagen) was added to Rneasy MinElute spin column, centrifuged (30 seconds, 8000g) and flow-through was discarded. 500 µl of 80% ethanol were added to the Rneasy MinElute spin column, centrifuged (2 minutes, 8000g) to wash the spin column membrane. The collection tube with flow-through was discarded. The Rneasy MinElute spin column was placed into a new 2 ml collection tube and centrifuged (5 minutes, 15000g). The collection tube with flow-through was discarded. The Rneasy MinElute spin column was placed into a new 1.5 ml collection tube and 14 µl of Rnase-free water was added directly to the centre of the spin column membrane. Sample was centrifuged (1 minute, 15000g). The concentration of obtained RNA was measured on NanoDrop spectrophotometer (ThermoFisher).

RNA was also isolated using Trizol reagent (ThermoFisher Scientific) and RNA clean & concentrator kit (Zymoresearch, R1013).

The cDNA transcription and amplification were done as described above (chapter 5.1.2.)

5.3.8 Quantitative Polymerase chain reaction (qPCR)

Obtained cDNA was diluted at least 25x for qPCR. 2 µl of cDNA were added to Absolute qPCR Plate Seal (ThermoFisher Scientific) which contained 3 µl of mix with primers and 2mM LightCycler Master Mix (Roche) (Table 8). The plate was centrifuged (1 minute, 800g) and put into LightCycler 480 Instrument II.

REAGENTS	VOLUME
H20	0 µl
Roche master mix	2.5 µl
PRIMER mix 3uM (F+R)	0.5 µl
DNA	2 µl
Final volume/well	5 µl

Table 8: Reaction for qPCR

Obtained qPCR data (C_t values) were normalized to data of reference qTCR and quantified. Raw data were acquired in The LightCycler® 480 Software 1.5 using Fit points analysis. Obtained C_t values (C_t value is a number of cycles required for a detection of a threshold amount of the amplified DNA.) were normalized to data of reference qTCR and quantified. cDNA used for qPCR was diluted 450x and 1000x. The efficiency of primers was calculated using Microsoft Excel.

5.4 Chemicals and antibodies

	Conjugate	Clone	Isotype	Reactivity	host	Company	Catalogue no
CD4	FITC	H129.19	IgG2a, κ	Mouse	Rat	BD Pharmingen	553651
CD8	APC	53-6.7	IgG2a, κ	Mouse	Rat	BD Pharmingen	553035
CD8a	BV421	53-6.7	IgG2a, κ	Mouse	Rat	Biolegend	558106
CD8	APC	MEM-31	IgG2a	Human	Mouse	Exbio	1A-027-T100
CD44	BV650	IM7	IgG2b, κ	Mouse	Rat	Biolegend	103049
CD69	Pe-Cy7	FN50	IgG1, κ	Human	Mouse	Biolegend	310912
B220	FITC	RA3-6B2	IgG2a, κ	Mouse	Rat	Biolegend	103206
CD90.1	Pe-Cy7	HIS51	IgG2a, κ	Mouse	Mouse	eBioscience	25-0900
TCR Vα2	PE	B20.1	IgG2a, λ	Mouse	Rat	Biolegend	127808
TCR Vα8	PE	B21.14	IgG1, κ	Mouse	Rat	Biolegend	127708
TCR Vβ5	APC	MR9-4	IgG1, κ	Mouse	Mouse	eBioscience	17-5796-82
TCRβ	APC	H57-597	IgG2, λ1	Mouse	Hamster	Biolegend	109212
MHC H-2Kb OVA	PE	25-D1.16	IgG1, κ	Mouse	Mouse	eBioscience	12-5743-82
Viability	APC-Cy7					Life Technologies	L34975
Viability	Hoechst 33258					ThermoFisher Scientific	H3569
DDAO	APC						

Table 9: table of used antibodies

Reagent	Company	Identifier
PBS 1x (8 g/l NaCl, 0.2 g/l KCl, 0.2 g/l KH2PO4, 1.15 g/l Na2HPO4)	IMG Core Facility – Media and Glass Washing	
Fetal Bovine Serum	Gibco	Cat# 102070
RPMI	Sigma Aldrich	Cat# R8758
D-MEM	Sigma Aldrich	Cat# D6429
IMDM	IMG Core Facility – Media and Glass Washing	
EDTA (10mM in PBS)	IMG Core Facility – Media and Glass Washing	
Penicillin potassium salt	BB Pharma	Reg# 15/156/69-A/C
Streptomycin sulfate salt	Sigma Aldrich	Cat# S9137
Gentamicin	Sandoz	Reg# 15/278/91-B/C
Ethanol absolute	VWR	Cat# 20823.293
LPS *E.Coli*	Sigma Aldrich	
OVA peptide (SIINFEKL)	Eurogentec	Ref# AS-60193-1
Brain Heart Infusion Agar	Sigma Aldrich	Cat# 70138
Brain Heart Infusion Broth	Sigma Aldrich	Cat# 53286
Trizol reagent	ThermoFisher Scientific	Cat# 5596026
EcoRI enzyme	ThermoFisher Scientific	Cat# ER0271
XhoI enzyme	ThermoFisher Scientific	Cat# ER0691
5X Reaction buffer	ThermoFisher Scientific	Cat# EP0441
Ribolock RNase inhibitor	ThermoFisher Scientific	Cat# EO0381
RevertAid reverse transcriptase	ThermoFisher Scientific	Cat# EP0441
5x HF buffer	New England Biolabs	Cat# M0530L
Phusion	New England Biolabs	Cat# M0530L
10x Cutsmart buffer	New England Bilabs	Cat# B7204S
CIP	New England Biolabs	Cat# M0290S
T4 DNA ligase enzyme	New England Biolabs	Cat# M0202S
Anti –FITC MicroBeads	MACS Miltenyi Biotec	Cat# 130-048-701
B-mercaptoethanol	Sigma Aldrich	Cat# 60-24-2

6 Results

6.1 Virtual memory T cells use a different TCR repertoire than naïve T cells

Previous studies showed the ability of CD8 T cells with higher self-reactivity receive enhanced homeostatic signals through their TCRs (26,73). White et al. (57) observed that the development of VM T cells might correlate with the expression of CD5, commonly used proxy for estimating the self-reactivity. However, the exact role of TCR specificity in the formation of VM $CD8^+$ T cells remained to be addressed.

Previous experiments performed in our laboratory showed that the strength of homeostatic TCR signals determine the T-cell fate decision where the decision is based on the level of self-reactivity of the T cell's TCR (data are shown in Fig. 1. in ref. 70). The correlation between the self-reactivity and the development of VM T cells leads us to the hypothesis that naïve and VM T cells might have distinct TCR repertoires and that these two subsets contain different TCR clonotypes.

To address our hypothesis we cloned and sequenced genes encoding for TCRα chains from OVA-reactive (Ovalbumin peptide SIINFEKL) $CD8^+$ VM and naïve T-cell subsets from germ-free Vβ5 mice. The experimental layout is shown in Fig. 3. Vβ5 mouse with fixed transgenic chain is biased towards the formation of CD8 T cells specific for Kb-OVA (~1% of all $CD8^+$ T cells) (74). Thus, the variability between the clones is limited to TCRα chains. By using primers specific for TRAV14 (TCRVα2) and TRAV12 (TCRVα8) TCR genes, we sequenced 12–20 clones in each group/experiment. We identified 44 clones from 4 independent experiments (Table 10). We focused on clonotypes (i.e., cells with the same amino acid sequence of CDR3 chain) that were repetitively present in two or more experiments. We observed significantly different distribution of certain clonotypes in VM and naïve T-cell repertoire. ‘VM clones’ were enriched among VM T cells and were also present in naïve T cells. In contrast, ‘naïve clones' were almost exclusively detected in naïve T cells (Fig. 4A) Subsequently, we observed different usage of TRAJ segments between VM and naïve T cells (Fig. 4B). In addition, we observed different genetics variants (different nucleotide setup of CDR3 chain) in the most abundant VM and naïve T-cell clones which suggesting independent development of each clone (Table 11).

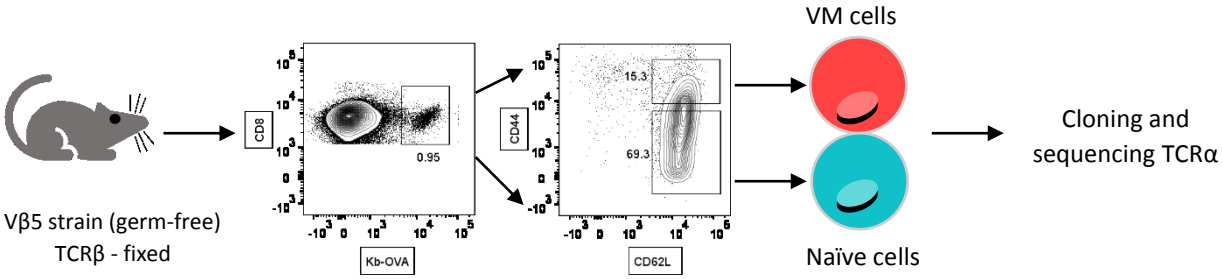

Fig. 3. Scheme of analysis of TCRα chain repertoire in Vβ5 mice

TCR clone	V-gene	J-gene	CDR3-junction	Clone count – naïve/VM			
				Exp1	Exp2	Exp3	Exp4
V14 clones				(19/18)	(16/16)	(21/17)	(17/17)
V14-c1	TRAV14-1 a) TRAV14D-1 TRAV14D-2	TRAJ6	CAAGGNYKPTF	-/9	-/10	12/12	1/8
V14-c2	TRAV14-1 b) TRAV14D-1	TRAJ6	CASGGNYKPTF	2/6	-/3	4/5	2/1
V14-c3	TRAV14-1	TRAJ6	CASGGNYQPIC	-/1	-	-	-
V14-c4	TRAV14-1	TRAJ6	CASGGNYKPTC	-/1	-	-	-
V14-c5	TRAV14-3	TRAJ5	CAASPQVVGQLTF	-/1	-	-	-
V14-c6	TRAV14-1 c) TRAV14D-3/DV8	TRAJ6	CAAGNYAQGLTF	2/-	7/-	4/-	-
V14-c7	TRAV14-1 d) TRAV14D-3/DV8	TRAJ31	CAAGDNNRIFF	4/-	-	-	3/-
V14-c8	TRAV14-1	TRAJ34	CAAGDTNKVVF	6/-	-	-	-
V14-c9	TRAV14-1	TRAJ47	CAASDPNKMIF	3/-	-	-	-
V14-c10	TRAV14-1	TRAJ33	CAASDNYQFIC	1/-	-	-	-
V14-c11	TRAV14-1	TRAJ31	CAAADNNRIFF	-	-/1	-	-
V14-c12	TRAV14-1 e)	TRAJ6	CAGGGNYKPTF	-	-/2	-	-
V14-c13	TRAV14-1	TRAJ7	CAASDNNRLTL	-	2/-	1/-	-
V14-c14	TRAV14-3	TRAJ43	CAASDNNNNAPRF	-	1/-	-	-
V14-c15	TRAV14-2	TRAJ35	CAARRGFASALTF	-	3/-	-	-
V14-c16	TRAV14-1	TRAJ33	CAAASNYQLIW	-	1/-	-	-
V14-c17	TRAV14-1	TRAJ31	CAASDDNRIFF	-	2/-	-	-
V14-c18	TRAV14D-3/DV8	TRAJ39	CAARDNAGAKLTF	1/-	-	-	-
V14-c19	TRAV14-1	TRAJ45	CAASAAGADRLTF	-	-	-	1/-
V14-c20	TRAV14-1	TRAJ6	CAASETSGGNYKPTF	-	-	-	1/-
V14-c21	TRAV14-2	TRAJ33	CAASGDSNYQLIW	-	-	-	2/-
V14-c22	TRAV14D-1	TRAJ6	CAVGGNYKPTF	-	-	-	1/-
V14-c23	TRAV14-1	TRAJ12	CAASEGGGYKVVF	-	-	-	1/-
V14-c24	TRAV14-1	TRAJ31	CAASDNNRIFF	-	-	-	2/-
V14-c25	TRAV14-1	TRAJ7	CAASDINRLTL	-	-	-	1/-
V14-c26	TRAV14D-1	TRAJ49	CAASSTGYQNFYF	-	-	-	1/-
V14-c27	TRAV14-1	TRAJ7	CAAGDNNRLTL	-	-	-	1/-
V14-c28	TRAV14-1	TRAJ6	CAAGGNYKPIF	-	-	-	-/1
V14-c29	TRAV14D-3/DV8	TRAJ52	CAASADTGANTGKLTF	-	-	-	-/2
V14-c30	TRAV14-2	TRAJ12	CAAWTGGYKVVF	-	-	-	-/1
V14-c31	TRAV14-1	TRAJ27	CAASDNTNTGKLTF	-	-	-	-/1
V14-c32	TRAV14-1	TRAJ6	CAAAGNYKPTF	-	-	-	-/1
V14-c33	TRAV14-1	TRAJ58	CAASAAGTGSKLSF	-	-	-	-/1

V12 clones				(17/18)	(20/12)	(18/16)	(20/15)
V12-c1	TRAV12N-3	TRAJ28	CALSVRLPGTGSNRLTF	-/2	-	-	-
V12-c2	TRAV12D-1	TRAJ23	CALSAEMNYNQGKLIF	-/2	-	-	-
V12-c3	TRAV12D-2	TRAJ27	CALSDRGTNTGKLTF	-/2	-	-	-/1
V12-c4	TRAV12N-3	TRAJ31	CALSGSNNRIFF	-/3	1/-	3/-	-
V12-c5	TRAV12N-3	TRAJ34	CAPTSNTNKVVF	-/1	-	-	-
V12-c6	TRAV12N-3	TRAJ28	CAPSIKMLTF	-/1	-	-	-
V12-c7	TRAV12N-3	TRAJ5	CALGTQVVGQLTF	-/1	-	-	-
V12-c8	TRAV12N-3	TRAJ28	CAPGSNRLTF	-/3	1/-	-	-
V12-c9	TRAV12-3 f) TRAV12D-2	TRAJ28	CALSETGTGSNRLTF	-/2	8/-	-	-
V12-c10	TRAV12D-2	TRAJ4	CALMLSGSFNKLTF	-/1	1/12	-/8	-
V12-c11	TRAV12D-2	TRAJ34	TNKVVF	3/-	-	7/-	17/1
V12-c12	TRAV12-3	TRAJ27	CALSDQGTNTGKLTF	2/-	-	3/-	-
V12-c13	TRAV12-3	TRAJ32	CALGMNYGSSGNKLIF	2/-	-	-	-
V12-c14	TRAV12-3	TRAJ52	CALSGGCGANTGKLTF	1/-	1/-	-	-
V12-c15	TRAV12N-3	TRAJ38	CALSRVGDYCKLIW	1/-	-	-	-
V12-c16	TRAV12-3	TRAJ31	CAPNSNNRIFF	1/-	-	-	-
V12-c17	TRAV12-3	TRAJ42	CALKGGSNAKLTF	1/-	-	-	-
V12-c18	TRAV12-3	TRAJ45	CAPLHTEGADRLTF	2/-	-	-	-
V12-c19	TRAV12N-3	TRAJ23	CALTGEMNYNQGKLIF	2/-	-	-	-
V12-c20	TRAV12-3	TRAJ50	CALSGPASSFSKLVF	1/-	-	-	-
V12-c21	TRAV12-3	TRAJ49	CALSPNTGYQNFYF	1/-	-	-	-
V12-c22	TRAV12-3	TRAJ27	CALSVPNTNTGKLTF	-	1/-	-	-
V12-c23	TRAV12-3	TRAJ5	CAPGTQVVGQLTF	-	1/-	-	-
V12-c24	TRAV12D-1	TRAJ32	CALSDGSSGNKLIF	-	2/-	-	-
V12-c25	TRAV12-3	TRAJ2	CALSVMNTGGLSGKLTF	-	1/-	1/-	-
V12-c26	TRAV12D-2	TRAJ4	CALSQESGSFNKLTF	-	1/-	-	-
V12-c27	TRAV12D-1	TRAJ42	CGLGGGSNAKLTF	-	1/-	-	-
V12-c28	TRAV12D-2	TRAJ25	CALSGVPGANTGKLTF	-	1/-	-	-
V12-c29	TRAV12D-2	TRAJ37	CALSDRRTGNTGKLIF	-	-	1/-	-
V12-c30	TRAV12N-3	TRAJ38	CALSRVGDNSKLIW	-	-	3/8	-
V12-c31	TRAV12-3	TRAJ27	CALSDIGTNTGKLTF	-	-	-	1/-
V12-c32	TRAV12D-2	TRAJ26	CALSDAAQGLTF	-	-	-	1/-
V12-c33	TRAV12D-25	TRAJ30	CALSADDTNAYKVIF	-	-	-	1/-
V12-c34	TRAV12D-2	TRAJ33	CALSDHNSNYQLIW	-	-	-	-/1
V12-c35	TRAV12D-2	TRAJ30	CALSSDTNAHKVIF	-	-	-	-/1
V12-c36	TRAV12D-2	TRAJ43	CALSGNNAPRF	-	-	-	-/2
V12-c37	TRAV12-3	TRAJ32	CALSDPYGSSGNKLIF	-	-	-	-/1
V12-c38	TRAV12N-3	TRAJ15	CAPYQGGRALIF	-	-	-	-/1
V12-c39	TRAV12N-3 g)	TRAJ23	CALSDRNYNQGKLIF	-	-	-	-/2
V12-c40	TRAV12-3	TRAJ42	CALGSNAKLTF	-	-	-	-/1
V12-c41	TRAV12-3	TRAJ42	CALRTQVVGQLTF	-	-	-	-/1
V12-c42	TRAV12-3	TRAJ27	CALSDRHTNTGKLTF	-	-	-	-/1
V12-c43	TRAV12N-3	TRAJ39	CALSDRYAGVILTF	-	-	-	-/1
V12-c44	TRAV12N-3	TRAJ34	CALSELSSNTNKVVF	-	-	-	-/1

Table 10: Distribution of TRAV14 and TRAV12 clones in four independent experiments

A

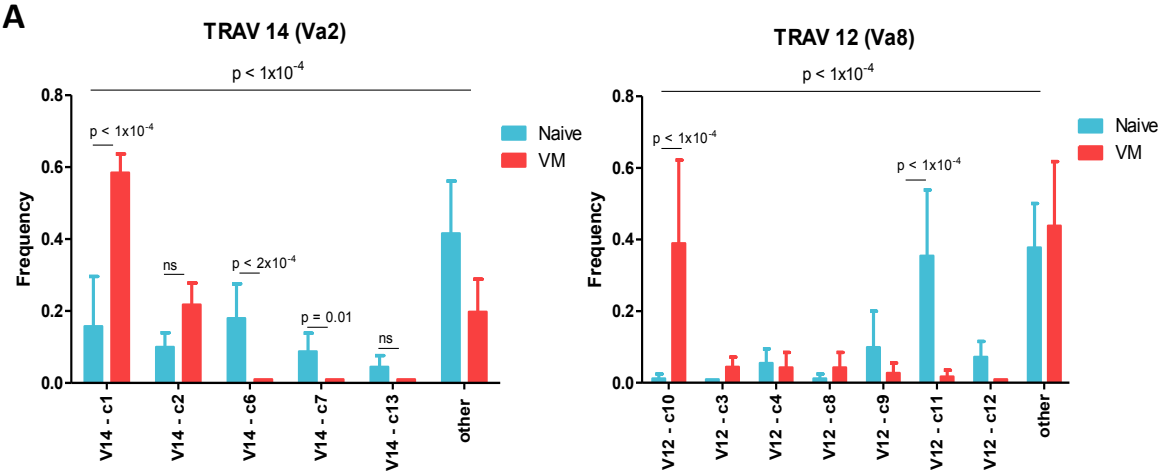

CLONOTYPE	CDR3	V-gene	J-gene
V14 – C1	CAAGGNYKPTF	TRAV14-1	TRAJ6
V14 – C2	CASGGNYKPTF	TRAV14-1	TRAJ6
V14 – C6	CAAGNYAQGLTF	TRAV14D-3DV8	TRAJ26
V14 – C7	CAAGDNNRIFF	TRAV14-1	TRAJ7
V14 – C13	CAASDNNRLTL	TRAV14-1	TRAJ7
V12 – C10	CALMLSGSFNKLTF	TRAV12D-2	TRAJ4
V12 – C11	TNKVVF	TRAV12D-2	TRAJ34

B

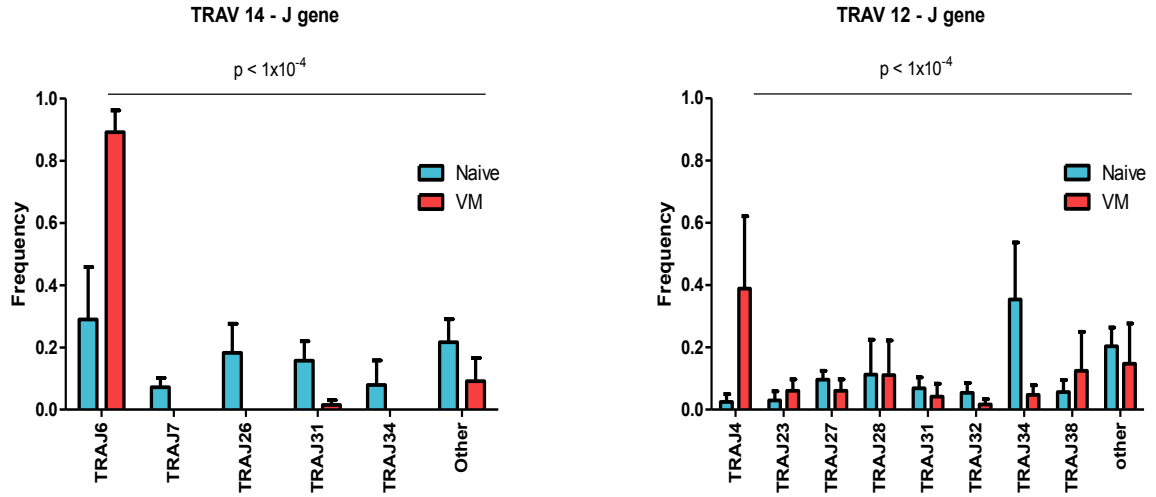

Fig. 4. Differences in the TCR repertoire between VM and naïve T-cell clones

A: RNA was isolated from memory ($CD44^+CD62L^+$) and ($CD44^+CD62L^+$) Kb-OVA^+ $4mer^+$ T cells sorted from LNs and the spleen of germ-free Vβ5 mice. TCRα encoding genes using either TRAV12 (corresponding to Vα8) or TRAV14 (corresponding to Vα2) were cloned and sequenced. 12–20 clones were sequenced in each group/experiment. Clonotypes identified in at least two experiments are shown. Mean frequency + SEM, n = 4 independent experiments. Statistical significance was determined by chi-square test (global test) and paired two-tailed T-tests as a post-test (individual clones). CDR3 sequences of clonotypes enriched in naïve or VM compartments are shown in the table.

B: TCRα sequences from Fig. 4A were analyzed for TRAJ usage. Means + SEM. n = 4 independent experiments. Statistical significance was determined by chi-square test.

TCR clone	V-gene	Genetic variant of the CDR3-junction	
V14-c1	TRAV14-1	A	tgtgca**gcgggg**ggaaactacaaacct**act**ttt
		B	tgtgca**gcagga**ggaaactacaaacct**act**ttt
		C	tgtgca**gccgga**ggaaactacaaacct**act**ttt
		D	tgtgca**gctgga**ggaaactacaaacct**act**ttt
		E	tgtgca**gcggga**ggaaactacaaacct**act**ttt
		F	tgtgca**gccggg**ggaaactacaaacct**acg**ttt
	TRAV14D-1	B	tgtgca**gcagga**ggaaactacaaacctacttttt
	TRAV14D-2	B	tgtgca**gcagga**ggaaactacaaacctacttttt
V14-c2	TRAV14-1	A	tgt**gct**tcaggaggaaactacaaacctacgttt
		B	tgt**gcc**tcaggaggaaactacaaacctacgttt
		C	tgt**gca**tcaggaggaaactacaaacctacgttt
		D	tgt**gcg**tcaggaggaaactacaaacctacgttt
	TRAV14D-1	C	tgt**gca**tcaggaggaaactacaaacctacgttt
		D	tgt**gcg**tcaggaggaaactacaaacctacgttt
V14-c6	TRAV14D-3/DV8	A	tgtgca**gcgggt**aactatgcccagggattaaccttc
		B	tgtgca**gcaggg**aactatgcccagggattaaccttc
	TRAV14-1	B	tgtgca**gcaggg**aactatgcccagggattaaccttc
V14-c12	TRAV14-1	A	tgt**gcc**gggggaggaaactacaaacctacgttt
		B	tgt**gcg**gggggaggaaactacaaacctacgttt
V12-c39	TRAV12N-3	A	tgtgctctgagtgat**cgg**aattataaccaggggaagctt atcttt
		B	tgtgctctgagtgat**agg**aattataaccaggggaagctt atcttt

Table 11: Genetic variant of the CDR3-junction

Collectively, our data suggest that TCR repertoire is distinct between VM and naïve T-cell subsets. We observed that only specific clonotypes have the potential to differentiation into VM T cells.

All these data are part of our recent publication "**Strong homeostatic TCR signals induce formation of self-tolerant virtual memory CD8 T cells**" (70).

6.2 TCRs from particular 'VM' and 'naïve clones' react differently to OVA peptide

In this part of thesis, we analyzed the signaling of particular OVA-reactive TCRs from the most abundant naïve and VM subsets that were cloned and sequenced as described above (chapter 6.1). To confirm that the TCRs cloned from Kb-OVA tetramer positive population respond to OVA, we expressed them in a widely used Jurkat $CD8^+$ cell line and characterize their response to OVA-loaded T2-Kb cells.

First, we cloned particular 'VM' and 'naïve clones' into retroviral pMSCV-GFP or pMSCV-LNGFR vectors and transduced them into Jurkat cell lines that expressed human CD8 and murine TCR Vβ5 chain. In the next step, we sorted GFP or LNGFR positive cells (Fig. 5A). We tried to sort multiple clones from both Vα2 and Vα8 groups. However, we were able to establish Jurkat cell line expressing only Vα2 clones for unknown reasons. Newly generated Jurkat cell lines were tested multiple times for their expression of surface markers. We measured expression of TCRβ – Vβ5, TCRα – Vα2 and CD8. We observed that the expression of these surface markers was comparable between all clones (Fig. 5B).

Next, we performed antigen presenting assay to measure the intrinsic response of particular clones. We used T2Kb cell line that expresses murine class I molecules as an antigen presenting cells and loaded them with different concentration of the OVA peptide. Then we added Jurkat cells expressing murine TCRs from either 'VM' or 'naïve clones' and analyzed the expression of activation marker CD69. The gating strategy is shown in Fig. 6A. We tested the responsiveness of 8 TCRs (i.e., 4 'VM clones' and '4 naïve clones') and observed that 6 clones responded to OVA whereas one 'VM clone' and one 'naïve clone' weren't reactive to OVA. Moreover, we observed the same non-responsiveness to OVA in a parallel ongoing experiments using primary cells that were performed in our laboratory (data not shown). Thence, that might be caused by different specificity of these TCRs. The examples of non-reactive clones are shown in Fig. 6B. Nonetheless, we had three functional 'VM clones' and three 'naïve clones' that were tested 3 – 8 times. The examples of the activation curves are shown in Fig. 6C.

We did two independent transfections using two different Jurkat cell lines (i.e., Jurkat $CD8^+$ OT-I TCRβ and LckKO $CD8^+$ OT-I TCRβ reintroduced with Lck containing FLAG tag). From each experiment, we analyzed EC50 values (i.e., the concentration of peptide that causes half-maximal response). We observed that TCRs generated from 'VM clones' are more reactive to OVA than TCRs from 'naïve clones'. We observed the same results in both Jurkat cell lines. However, the response of clones expressed in Jurkat $CD8^+$ OT-I TCRβ cell line (Fig. 7A) was more sensitive than the response in reconstituted Jurkat cell line with Lck Flag (Fig. 7B). The observation that Jurkat $CD8^+$ OT-I TCRβ cell line is more sensitive correlates with other experiments that were performed in our laboratory (data not shown). Next, we stained all clones with the Kb-OVA tetramer and surprisingly we observed the correlation with EC50 values. The more self-reactive 'VM clones' had better binding to tetramer than less self-reactive 'naïve clones' (Fig. 8A), although the expression of TCRα, TCRβ, and CD8 was comparable (Fig. 5B). However, tetramer binding in primary cells was comparable for all the clones (data not shown) which indicates that the differences in binding might be caused by Jurkat system and it shouldn't be caused by TCRs themselves. One possible explanation is that 'naïve clones' bind to endogenous TCR of Jurkat cells.

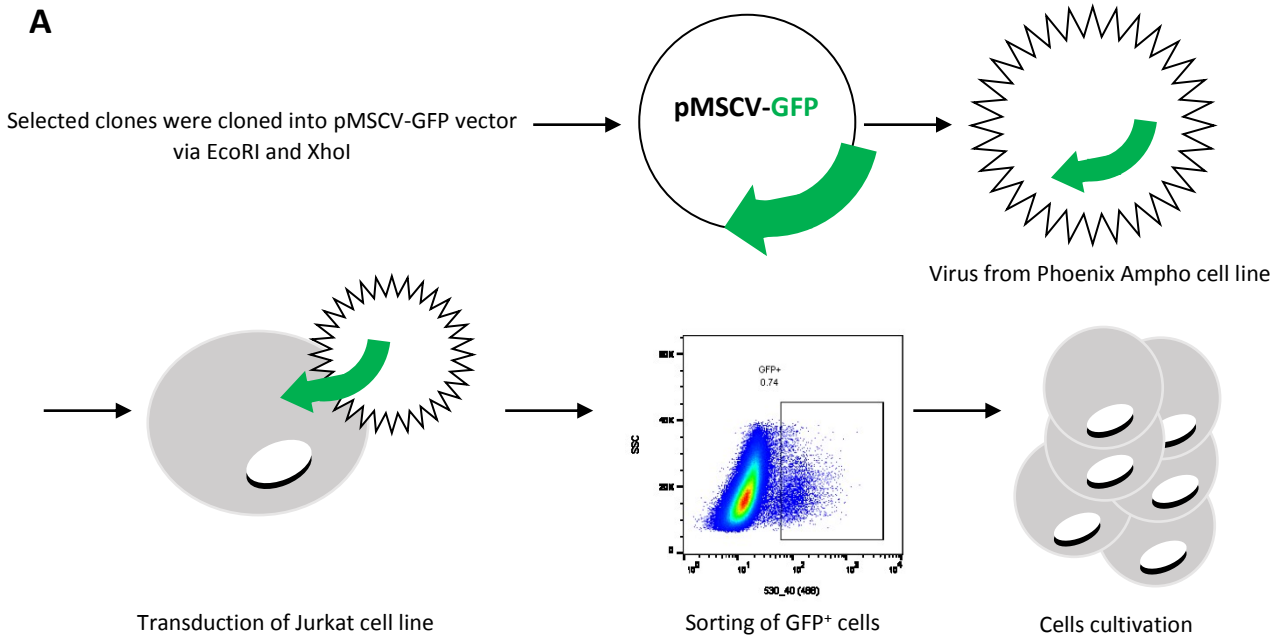

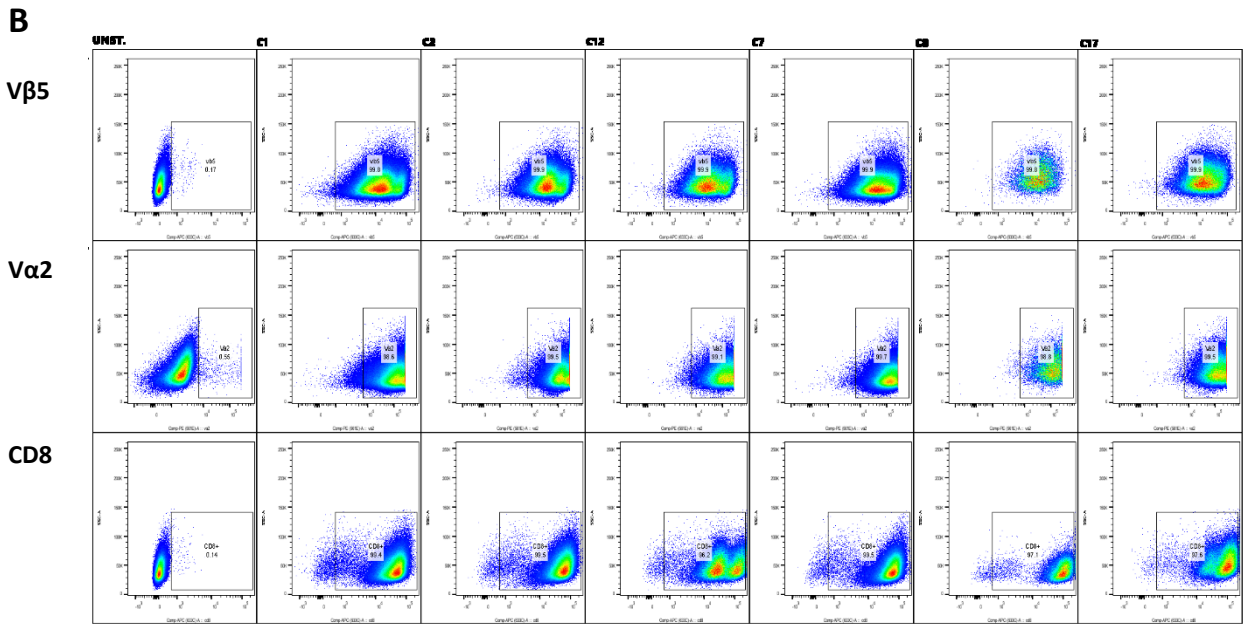

Fig. 5. Generation of Jurkat cell line expressing Vα2 'VM' and 'naïve clones'
A: Schematic representation of generation of Jurkat cell line expressing GFP⁺ clones.
B: Flow cytometry analysis of the T-cell surface markers. C1, C2, and C12 are 'VM clones'. C7, C8, and C17 are 'naïve clones'.

A

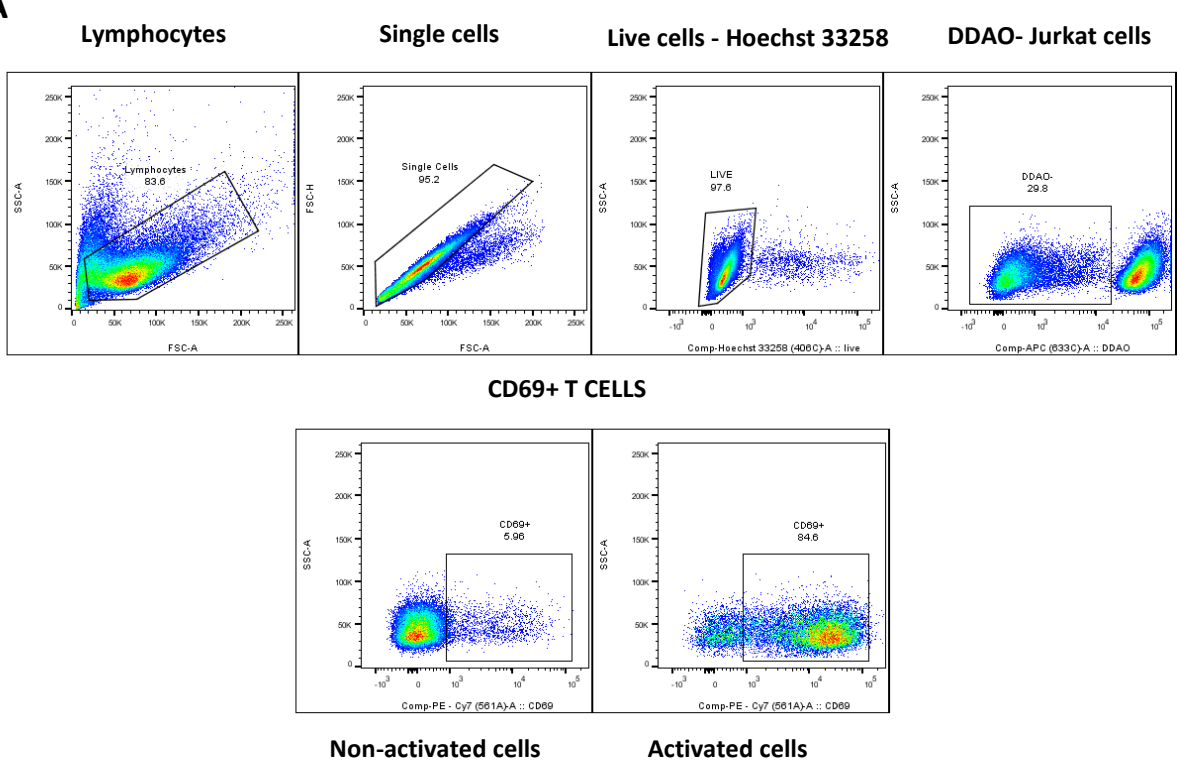
Lymphocytes
Single cells
Live cells - Hoechst 33258
DDAO- Jurkat cells
Lymphocytes
83.6
Single Cells
95.2
LIVE
97.6
DDAO-
29.8
SSC-A
FSC-A
FSC-H
Comp-Hoechst 33258 (406C)-A :: live
Comp-APC (633C)-A :: DDAO
CD69+ T CELLS
CD69+
5.96
CD69+
84.6
Comp-PE - Cy7 (561A)-A :: CD69
Non-activated cells
Activated cells

B

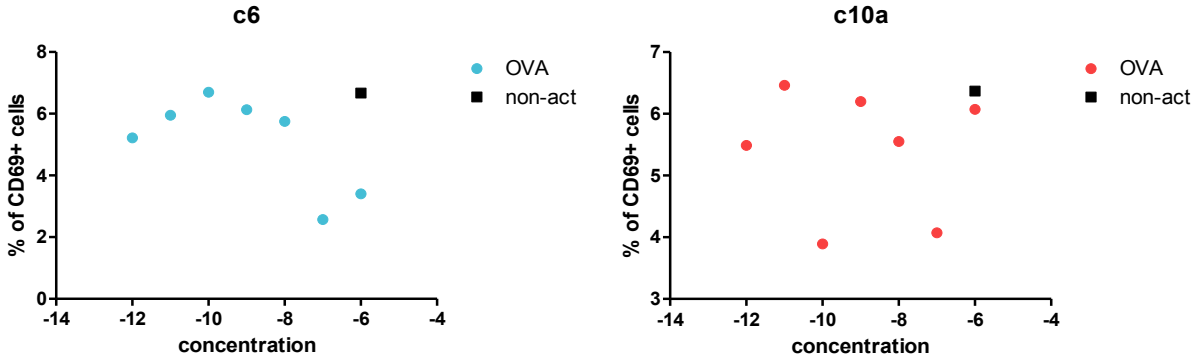
c6
c10a
% of CD69+ cells
concentration
OVA
non-act

C

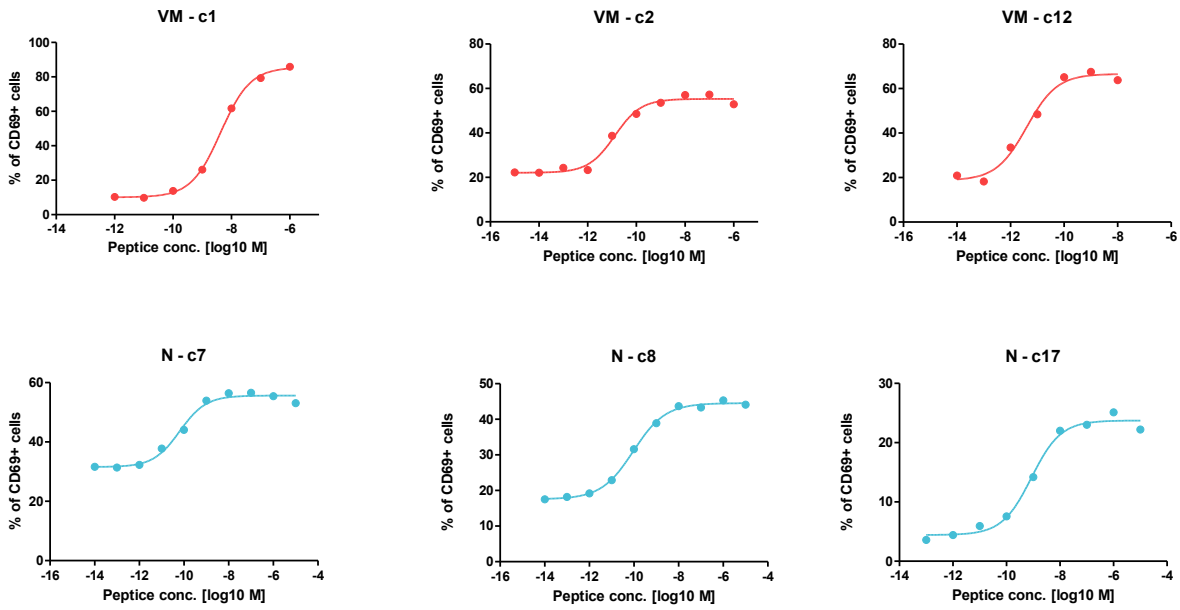

Fig. 6.: Analysis of CD69⁺ T cells

A: Gating strategy.

B, C: Quantification of the experiments. Y axis indicates the percentage of CD69⁺ cells. X axis indicates concentration of peptide. The % of cells were fitted against concentration in log scale in GraphPad Prism. **B:** The example of non-reactive clones. C6 is 'naïve clone', c10 is 'VM clone' **C:** Representative concentration curves for three 'VM clones' (red) and three 'naïve clones' (blue). Curves were fit using nonlinear regression and EC50 values were calculated.

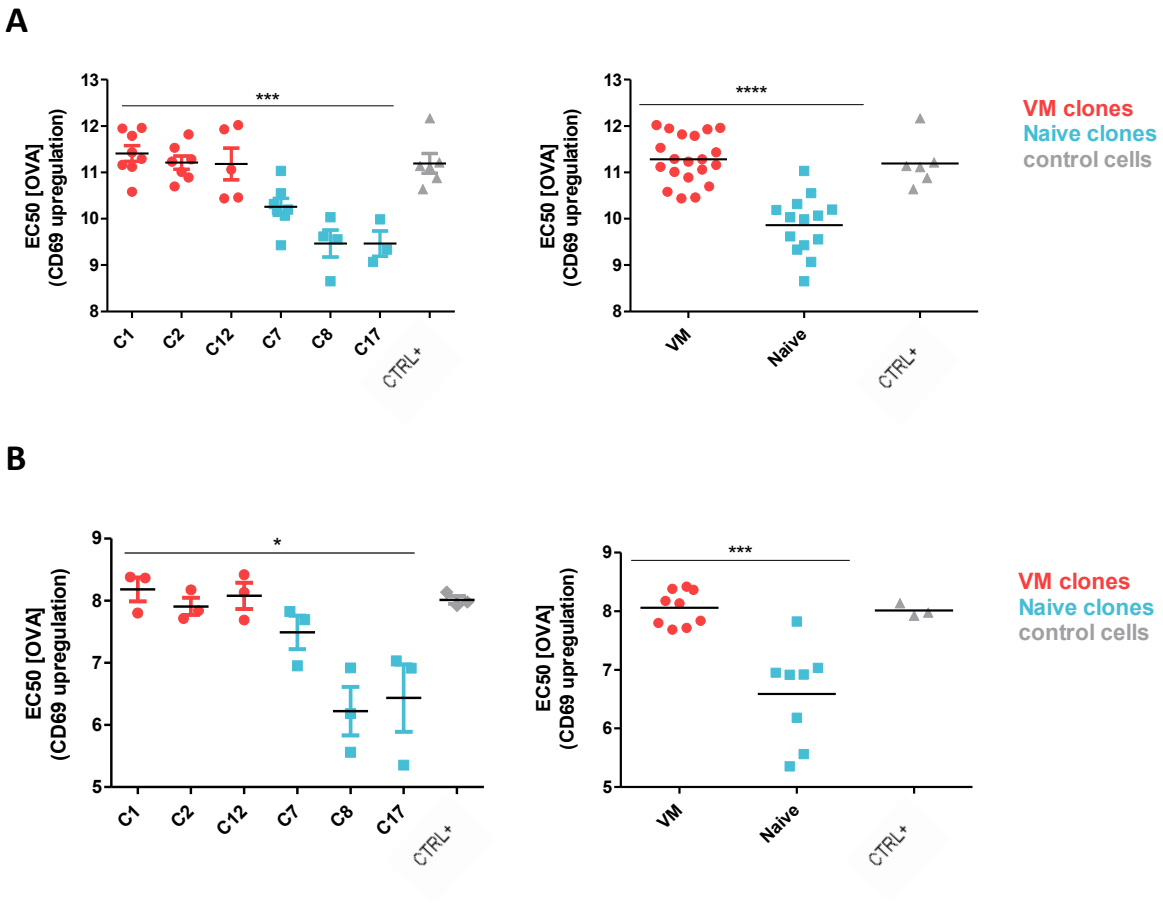

Fig. 7.: Virtual memory T-cell clones are more reactive to OVA than naïve T-cell clones

A, B: EC50 values of particular clones are shown in the left panel. EC50 values for VM (red dots) and naïve (blue dots) group are shown in the right panel. Control T cells that are responsive to OVA are grey. T-cell clones were tested 3 – 8 times in two independent experiments using different Jurkat cell lines. Statistical significance was determined using Kruskal–Wallis test (left panel) and Mann-Whitney test (right panel). For each figure, significant differences between groups are indicated by P values. Shown are mean ± SEM. **A:** 1st transfection – Jurkat $CD8^+$ OTI TCRβ cells, clones with GFP**.** P-value representation: *** < 0.002 (left panel) **** < 0.0001 (right panel). **B:** 2nd transfection – Lck Flag $CD8^+$ OTI TCRβ cells, clones with LNGFR. P-value representation: * < 0.0272 (left panel) *** < 0.0006 (right panel).

A

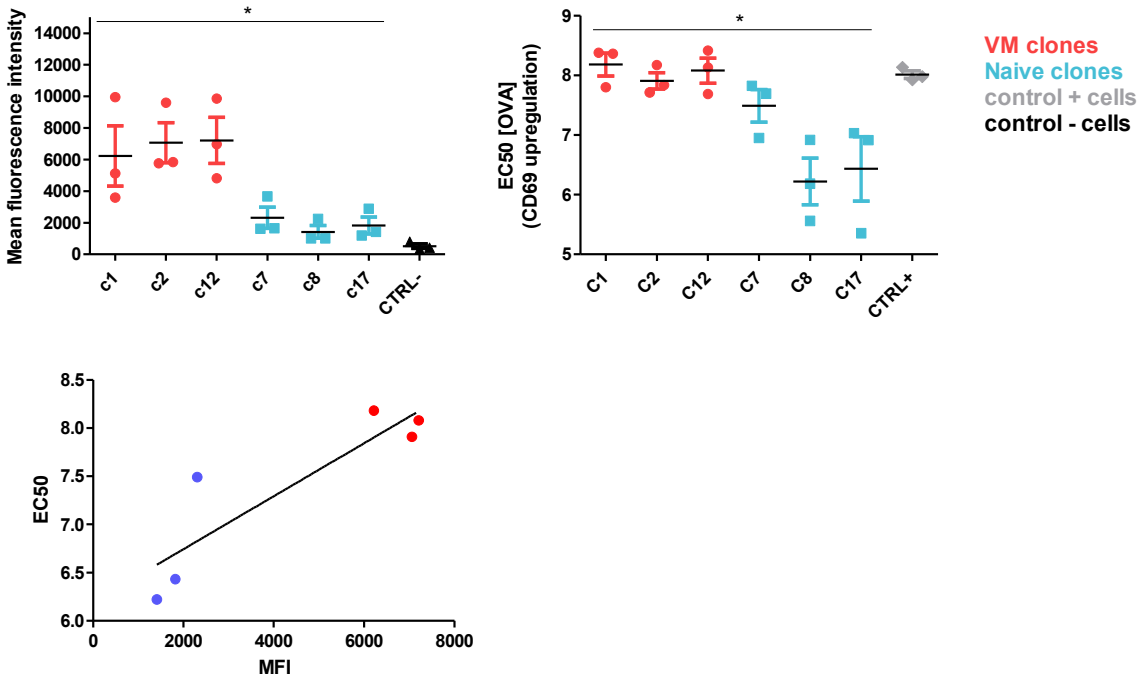

Fig. 8.: Different OVA-tetramer binding of particular OVA-reactive TCRs

A: Particular 'VM clones' and 'naïve clones' were stained with Kb-OVA and analyzed on FACS. The staining was done 3 times for each clone. Statistical significance was determined using Kruskal-Wallis test. Y axis indicates Mean fluorescence intensity (MFI). Red dots represent 'VM clones'. Blues dots represent 'naïve clones'. Black dots represent negative control cells that don't bind to Kb-OVA (left upper panel). For comparison, in the right upper panel are EC50 values. Statistical significance was determined using Kruskal-Wallis test. P-value representation: * < 0.0234 (left upper panel) * < 0.0272 (right upper panel). Shown are mean ± SEM. In the left bottom panel is linear correlation between EC50 (Y axis) and Mean fluorescence intensity (X axis). Blue dots represent 'naïve clones' and red dots represent 'VM clones'. R-square: 0.7785.

Taken together, in this part of the thesis we successfully expressed several functional TCRs from both subsets that were reactive to OVA in two Jurkat cell lines. We observed different responsiveness to peptide between ‘naïve’ and ‘VM clones’. The more self-reactive ‘VM clones’ reacted to OVA better than less self-reactive ‘naïve clones’ in both used Jurkat cell lines. These results might indicate that TCRs from ‘naïve clones’ interfered with endogenous TCR of Jurkat cells.

6.3 qPCR – based method for detection of particular OVA-reactive clones

In this part of thesis, we aimed to develop a relatively simple qPCR-based method to monitor the abundance of particular T-cell clonotypes (i.e., 'VM clones' and 'naïve clones') during the immune response.

It is technically demanding to monitor the behaviour of naïve and VM T cells during the course of the immune response because after activation we can no longer recognize which clones were originally VM and which were naïve. One possibility how to monitor it, is to generate monoclonal populations of naïve and VM T cells, adoptively transfer them into a congenic host, and detect them based on the congenic markers (70). Another possibility would be the analysis of the TCR repertoires from various time points during the course of the immune response. However, both of these approaches are technically and financially demanding.

qPCR-based method would be relatively versatile to quantify particular clonotypes at different time points, in different sorted T-cell subset, or in different organs. In particular, the method was planned for the detection of the relative abundance of clonotypes with a low and high level of self-reactivity, respectively, during the onset of immune responses in the various organs.

First, we designed primers using TCRα sequences from one 'VM' and one 'naïve' OVA-specific clones from Vβ5 mice that were cloned and sequenced as described above (chapter 6.1) (70). As the Vβ5 mouse contains the fixed transgenic TCRβ chain, the TCRα is the only source of clonal variability (74). Multiple pairs of primers were designed to at least partially bind into the hypervariable CDR3 motif and to amplify segment between TRAV14 and TRA6 for the 'VM clone' (Fig. 9A) and between TRAV14 and TRAJ31 for the 'naïve clone' (Fig. 9B). Because of the sequence similarities between the most abundant TRAV14 'VM clones' and because of the TRAJ usage differences between 'naïve clones' and 'VM clones' (70), such primers might have a potential to discriminate groups of naïve (weak self-reactivity) and VM (strong self-reactivity) clonotypes.

Next, we tested the pairs of primers for their efficiency and functionality. For this validation, we used plasmids containing 'VM' and 'naïve clones' (i.e., 'VM TCR' and 'naïve TCR'). C_t values (i.e., the number of cycles required for a detection of a threshold amount of the amplified DNA) were plotted against the logarithm of concentration to determine the efficiency of the particular primer pair. As a control primer pair, we used previously tested 'qTCRα primer' that was designed to amplify the constant region of TCRα. We chose two pairs of 'VM primers' and two pairs of 'naïve primers' based on their efficiency (Table 12). The C_t values are shown in Fig. 10A. These data showed that pairs of primers that were designed for the detection of 'VM T-cell clones' or 'naïve T-cell clones' have indeed the preference for the 'VM TCR' or the 'naïve TCR', respectively. The representative amplification curves of pair of 'VM primer 2' and pair of 'naïve primer 1' on both templates are shown in Fig. 10B, C.

In a next step, we tested whether the 'VM primers' and 'naïve primers' have the expected preference for VM and naïve Kb-OVA$^+$ Vβ5 T cells, respectively. We isolated RNA from sorted Kb-OVA$^+$ CD44$^+$ (mostly VM) and CD44$^-$ (naïve) CD8$^+$ T cells sorted from the spleen of Vβ5 mice (74). The gating strategy is shown in Fig. 11A. Then we synthesised cDNA from the RNA for the validation of the primers. For the qPCR the cDNA was diluted 450x and 10000x. As a negative control we used no template control which usually had C_t around 33 – 34 or had no signal at all. The C_t values are shown in Fig. 11B. As we expected, primers designed for either 'VM clones' or 'naïve clones' had lower C_t values in CD44$^+$ T cells and CD44$^-$ T cells, respectively. We saw the same results in both used dilutions. The representative amplification curves of pair of 'VM primer 2' and pair of 'naïve primer 1' are shown in Fig. 11C, D.

After we established the method enabling the discrimination between 'VM' and 'naïve clones', we proceeded to use it for the relative quantification of 'VM' and 'naïve clones' prior to and during the immune response. First, we immunized Vβ5 mice with OVA-loaded DCs, but we failed to detect the reproducible expansion of OVA-loaded CD8$^+$ T cells in this assay (data not shown).

Using a modified protocol, we immunized the mice with *Listeria monocytogenes* expressing OVA (Lm-OVA). We had one group of Vβ5 mice that were not immunized, and one group of mice immunized with Lm-OVA for 3 days. We isolated RNA from $CD8^+$ Kb-OVA^+ T cells. The representative gating strategy for immunized and non-immunized mice is shown in Fig. 12A. Then we synthesised cDNA from RNA. The C_t values are shown in Fig. 12B. Difference in cycles between cDNA from immunized and non-immunized mice was converted to fold-change. The data were analyzed using relative quantification where all C_t values were normalized relative to reference 'qTCR primer' pair and cDNA from immunized mice was relative to non-immunized cDNA. As we expected, 'VM clones' were enriched during the initial infection compared to 'naïve clones' (Fig. 12C).

A

'VM clone'

Result summary:	Productive TRA rearranged sequence: (no stop codon and in-frame junction)		
V-GENE and allele	Musmus TRAV14-1*01 F, or Musmus TRAV14N-1*01 F	score = 1370	identity = 100.00% (275/275 nt)
J-GENE and allele	Musmus TRAJ6*01 F	score = 275	identity = 100.00% (55/55 nt)
FR-IMGT lengths, CDR-IMGT lengths and AA JUNCTION	[26.17.34.11]	[6.7.9]	CAAGGNYKPTF

ACGTTTTTACTCCTAGGCCTTCACCTAGCTGGGGTGAATGGCCAGCAGCAGGAGAAACGTGACCAGCAGCAG
GTGAGACAAAGTCCCCAATCTCTGACAGTCTGGGAAGGAGAGACCGCAATTCTGAACTGCAGTTATGAGGAC
AGCACTTTTAACTACTTCCCATGGTACCAGCAGTTCCCTGGGGAAGGCCCTGCACTCCTGATATCCATACGTTCA
GTGTCCGATAAAAAGGAAGATGGACGATTCACAATCTTCTTCAATAAAAGGGAGAAAAAGCTCTCCTTGCACA
TCACAGACTCTCAGCCTGGAGACTCAGCTACCTACTTC**TGTGCAGCAGGAGGAAACTACAAACCTACGTTTG**G
GAAAGGGACCAGCCTCGTGGTTCATCCATACATCCAGAACCCAGAACCTGCTGTGTACCAGTTAAAAGATCCT
CGGTCTCAGGACAGCACCCTCTGCCTGTTCACCGACTTTGACTCCCAAATCAATGTGCCGAAAACCATGGAATC
TGGAACGTTCATCACTGACAAAACTGTGCTGGACATGAAAGCTATGGATTCCAAGAGCAATGGGGCCATTGCC
TGGAGCAACCAGACAAGCTTCACCTGCCAAGATATCTTCAAAGAGACCAACGCCACCTACCCCAGTTCAGACG
TTCCCTGTGATGCCACGTTGACTGAGAAAAGCTTTGAAACAGATATGAACCTAAACTTTCAAAACCTGTCAGTT
ATGGGACTCCGAATCCTCCTGCTGAAAGTAGCCGGATTTAACCTGCTCATGACGCTGAGGCTGTGGTCCAGTT
GAGAATTCCTGCAGCCCGGGGGATCCACTAGTTCTAGAGCGGCCGCCACCGCGGTGGAGCTCCAGCTTTTGTT
CCCTTTAGTGAGGGTTAATTGCGCGCT

B

'Naïve clone'

Result summary:	Productive TRA rearranged sequence: (no stop codon and in-frame junction)		
V-GENE and allele	Musmus TRAV14-1*01 F, or Musmus TRAV14N-1*01 F	score = 1370	identity = 100.00% (275/275 nt)
J-GENE and allele	Musmus TRAJ31*02 F	score = 239	identity = 92.73% (51/55 nt)
FR-IMGT lengths, CDR-IMGT lengths and AA JUNCTION	[26.17.34.11]	[6.7.9]	CAAGDNNRIFF

GAGATGGACAGATCCTGACAGCAACGTTTTTACTCCTAGGCCTTCACCTAGCTGGGGTGAATGGCCAGCAGCA
GGAGAAACGTGACCAGCAGCAGGTGAGACAAAGTCCCCAATCTCTGACAGTCTGGGAAGGAGAGACCGCAAT
TCTGAACTGCAGTTATGAGGACAGCACTTTTAACTACTTCCCATGGTACCAGCAGTTCCCTGGGGAAGGCCCTG
CACTCCTGATATCCATACGTTCAGTGTCCGATAAAAAGGAAGATGGACGATTCACAATCTTCTTCAATAAAAGG
GAGAAAAAGCTCTCCTTGCACATCACAGACTCTCAGCCTGGAGACTCAGCTACCTACTTC**TGTGCAGCAGGGG**
ACAATAACAGAATCTTCTTTGGTGATGGGACGCAGCTGGTGGTGAAGCCCAACATCCAGAACCCAGAACCTG
CTGTGTACCAGTTAAAAGATCCTCGGTCTCAGGACAGCACCCTCTGCCTGTTCACCGACTTTGACTCCCAAATCA
ATGTGCCGAAAACCATGGAATCTGGAACGTTCATCACTGACAAAACTGTGCTGGACATGAAAGCTATGGATTC
CAAGAGCAATGGGGCCATTGCCTGGAGCAACCAGACAAGCTTCACCTGCCAAGATATCTTCAAAGAGACCAAC
GCCACCTACCCCAGTTCAGACGTTCCCTGTGATGCCACGTTGACTGAGAAAAGCTTTGAAACAGATATGAACCT
AAACTTTCAAAACCTGTCAGTTATGGGACTCCGAATCCTCCTGCTGAAAGTAGCCGGATTTAACCTGCTCATGA
CGCTGAGGCTGTGGTCCAGTTGAGAATTCCTGCAGCCCGGGGGATCCACTAGTTCTAGAGCGGCCGCCACCGC
GGTGGAGCTCCAGCTTTTGTTCCCTTTAGTGAGGGTTAATTGCGCGCTTGGCGTAATCATGGTCATAGCTGTTT
CCTGTGTGAAATTGTTATCCGCTCACAATTCCACACAACATACGAGCCGGAAGCATAAAGTGTAAAGCCTGGG
GTGCCTAATGAGTGAGCTAACTCACATTAATTGCGTTGCGCTCACTGC

Fig. 9.: Sequences of 'VM' and 'naïve clones' used for primers design
Sanger sequences were analyzed using SeqMan Pro.
A: 'VM clone': The yellow part showing TRAV14 segment, the green part showing TRAJ6 segment, the underline segment showing CDR3 motif. **B:** 'Naïve clone': The yellow part showing TRAV14 segment, the green part showing TRAJ31 segment, the underline segment showing CDR3 motif.

PRIMER NAME	5′ → 3′ sequence
VM1_F	AGGCCCTGCACTCCTGATA
VM1_R	TGTATGGATGAACCACGAGGC
VM2_F	AGGCCCTGCACTCCTGATA
VM2_R	TATGGATGAACCACGAGGCTG
N1_F	TTCTGGATGTTGGGCTTCACCA
N1_R	GGAGAAAAAGCTCTCCTTGCAC
N2_F	CTCTCCTTGCACATCACAGACT
N2_R	GGATGTTGGGCTTCACCACC
qTCRα_F	ACATCCAGAACCCAGAACCTG
qTCRα_R	AAAGTCGGTGAACAGGCAGA

Table 12: Chosen primers used for qPCR

A

	'VM PRIMER 1'			'NAÏVE PRIMER 1'	
	C_t values			**C_t values**	
	VM TCR clone	*Naïve TCR clone*		*VM TCR clone*	*Naïve TCR clone*
MEDIAN	12.86	23.39	**MEDIAN**	29.76	16.69
	'VM PRIMER 2'			'NAÏVE PRIMER 2'	
	C_t values			**C_t values**	
	VM TCR clone	*Naïve TCR clone*		*VM TCR clone*	*Naïve TCR clone*
MEDIAN	14.38	24.79	**MEDIAN**	26.83	16.84

B

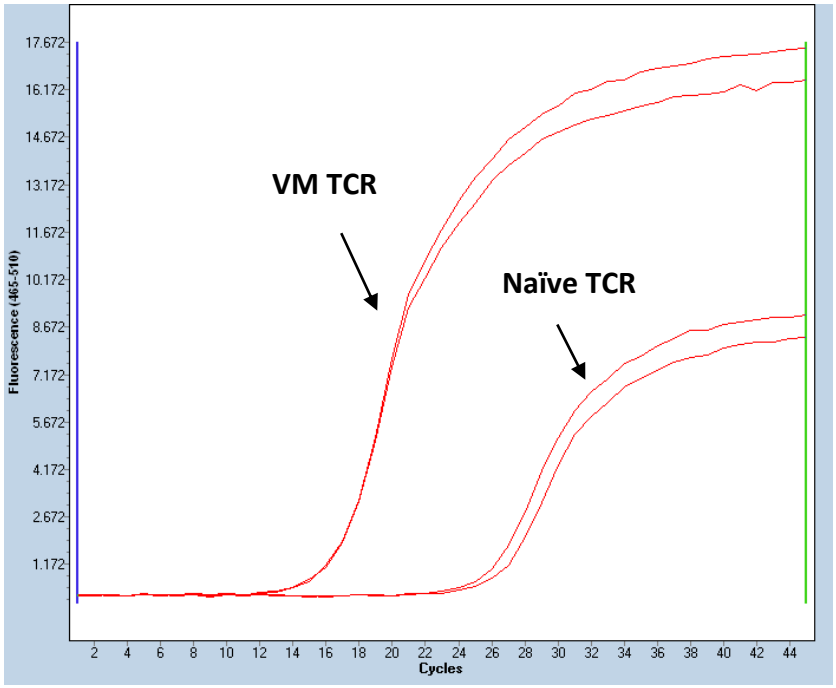

C

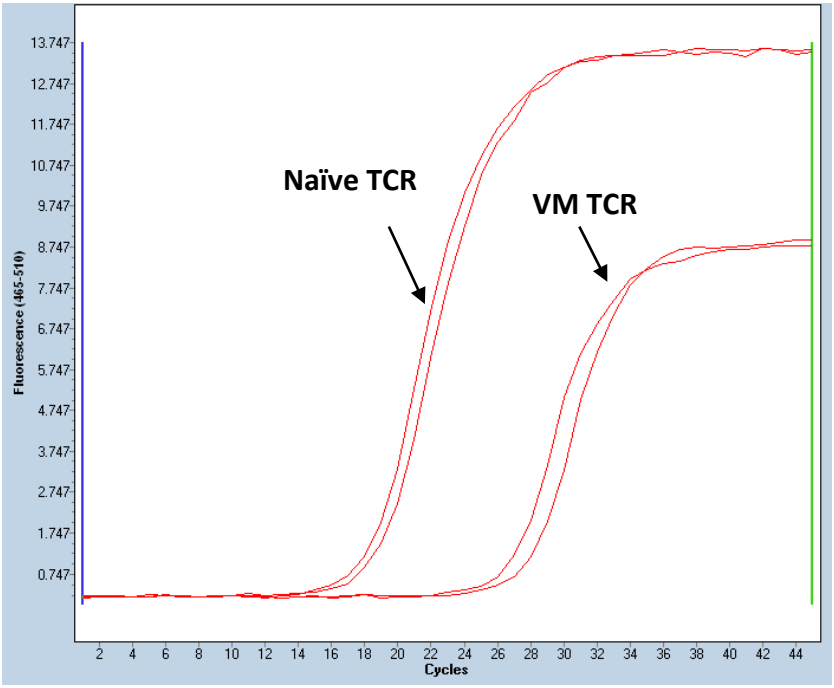

Fig. 10.: The quantification analysis using the LightCycler® 480 System

A: Median C_t values of two technical replicates for each pair of primers. C_t values were calculated in The LightCycler® 480 Software 1.5 using Fit points analysis. **B, C:** Amplification curves of 'VM' and 'naïve TCR' using pair of primers ('VM2' (B) and 'N1' (C) primer) designed for the amplification of either 'VM clones' or 'naïve clones'. Two technical replicates for each curve are shown.

A

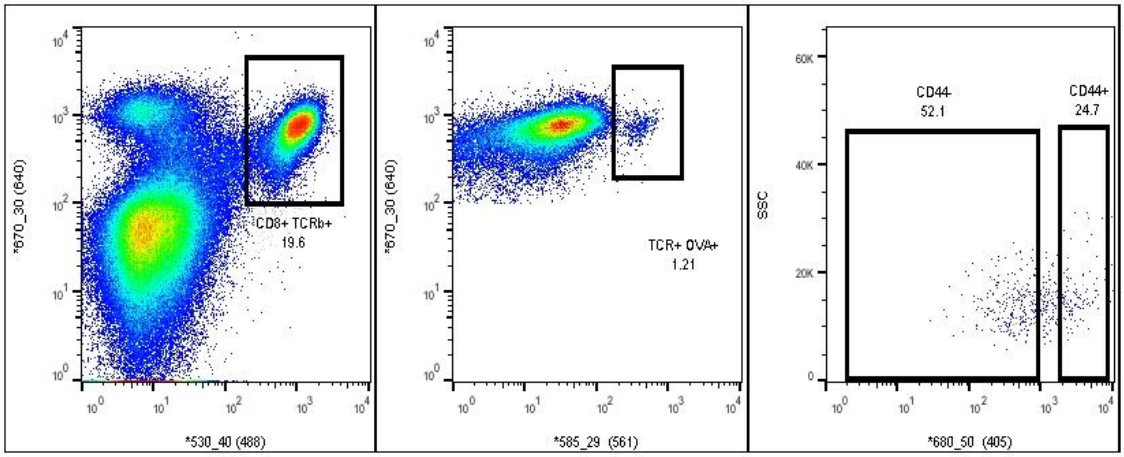

$CD8^+ TCR\beta^+$ ⟶ $TCR\beta^+ Kb\text{-}OVA^+$ ⟶ $CD44^- CD44^+$

B

'VM PRIMER 1'				
	C_t values			
	VM cDNA 450x	*Naïve cDNA 450x*	*VM cDNA 10000x*	*Naïve cDNA 10000x*
MEDIAN	12.65	15.61	17.35	20.54
'VM PRIMER 2'				
	C_t values			
	VM cDNA 450x	*Naïve cDNA 450x*	*VM cDNA 10000x*	*Naïve cDNA 10000x*
MEDIAN	12.61	15.69	17.1	20.15
'NAÏVE PRIMER 1'				
	C_t values			
	VM cDNA 450x	*Naïve cDNA 450x*	*VM cDNA 10000x*	*Naïve cDNA 10000x*
MEDIAN	16.49	13.82	21.44	18.60
'NAÏVE PRIMER 2'				
	C_t values			
	VM cDNA 450x	*Naïve cDNA 450x*	*VM cDNA 10000x*	*Naïve cDNA 10000x*
MEDIAN	16.51	13.89	21.23	18.57
'qTCR PRIMER'				
	C_t values			
	VM cDNA 450x	*Naïve cDNA 450x*	*VM cDNA 10000x*	*Naïve cDNA 10000x*
MEDIAN	12.52	11.49	17.50	16.15

C

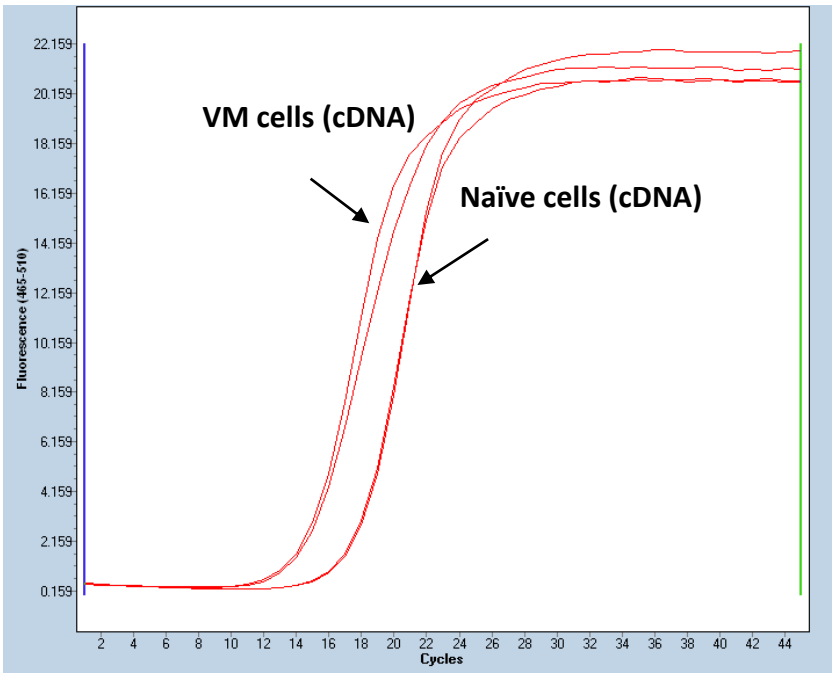

D

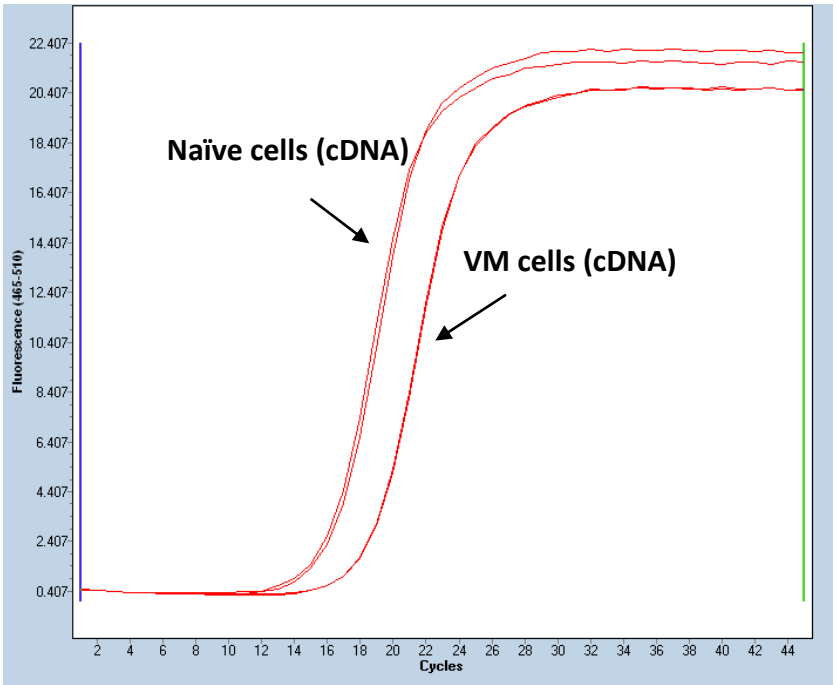

Fig. 11.: Validation of primers using cDNA from CD44$^+$ and CD44$^-$ T cells.
A: The gating strategy for sort.
B: Median C_t values of two technical replicates for each pair of primers. C_t values were calculated in The LightCycler® 480 Software 1.5 using Fit points analysis. **C, D:** Amplification curves of CD44$^+$ and CD44$^-$ cDNA using pair of primers ('VM2' (C) and 'N1' (D) primer) designed for the amplification of either 'VM clones' or 'naïve clones'. The curves showing amplification of cDNA that was diluted 450x. Two technical replicates for each curve are shown.

A

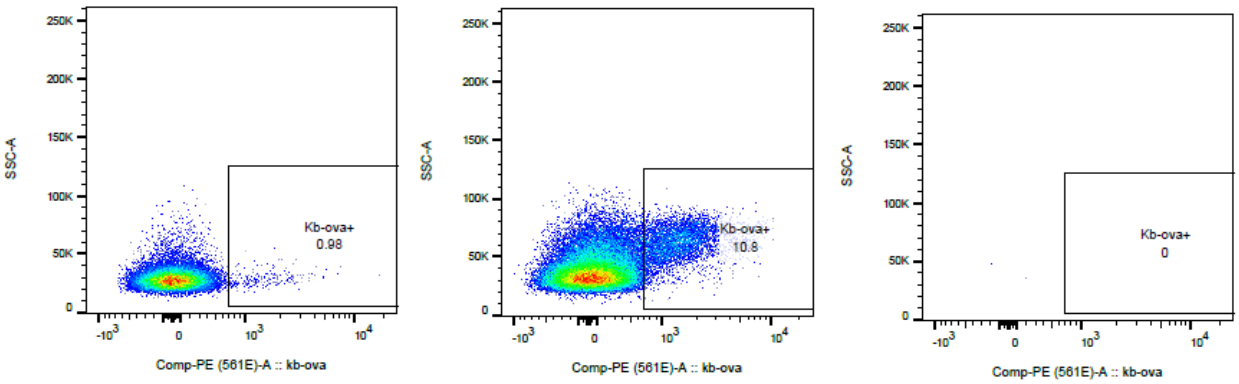

Kb-OVA$^+$ cells from control Vβ5 mouse

Kb-OVA$^+$ cells from Lm-OVA infected Vβ5 mouse

Unstained control cells

B

	‘VM PRIMER 1‘	
	C_t values	
	post-infection (cDNA)	*pre-immunization (cDNA)*
MEDIAN	9.68	12.57
	‘VM PRIMER 2‘	
	C_t values	
	post-infection (cDNA)	*pre-immunization (cDNA)*
MEDIAN	9.47	12.00
	‘NAÏVE PRIMER 1‘	
	C_t values	
	post-infection (cDNA)	*pre-immunization (cDNA)*
MEDIAN	13.28	14.89
	‘NAÏVE PRIMER 2‘	
	C_t values	
	post-infection (cDNA)	*pre-immunization (cDNA)*
MEDIAN	13.51	15.38
	‘qTCR PRIMER‘	
	C_t values	
	post-infection (cDNA)	*pre-immunization (cDNA)*
MEDIAN	10.32	12.28

C

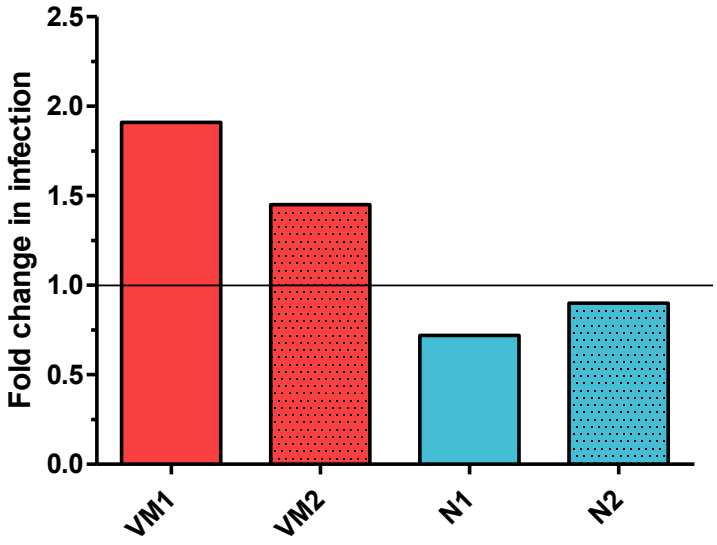

Fig. 12: Lm-OVA Vβ5 analysis on day 3

A: The representative gating strategy of immunized mouse and non-immunized mouse. The mice were staining with Kb-OVA and analyzed three days after infection on FACS. **B:** Median C_t values of three technical replicates for each pair of primers. C_t values were calculated in The LightCycler® 480 Software 1.5 using Fit points analysis. **C:** The fold-change of cDNA from immunized mice relative to cDNA from non-immunized mice. All C_t values were normalized to control 'qTCR' primer pair. The red columns represent pairs of 'VM primers'. The blue columns represent pairs of 'naïve primers'. The enrichment of 'VM clones' is more than 1x compared to 'naïve clones'.

In summary, in this part we developed and optimized a qPCR-based method for the detection of particular group of OVA-reactive clones. We designed several pairs of primers which amplified TCRs from particular group of T cells clones.

This method will serve as a tool for the analysis of the expansion and organ infiltration of particular group of clones during the course of infection.

7 Discussion

Recent studies reported the existence of the T-cell compartment that contains memory phenotype T cells that have not encountered their foreign cognate antigen previously. These T cells that occur in healthy non-manipulated lymphoreplete mice were termed virtual memory $CD8^+$ T cells and constitute 10–20% of all peripheral $CD8^+$ T cells in mice (56,67,69). However, their formation is still incompletely understood. One possible explanation is that VM T cells might be formed purely on a stochastic basis or during newborn lymphopenia (67). Another pilot studies suggested that the important role in the formation of VM T cells might have TCR specificity (57,62).

In the first part of this thesis, we wondered whether or not VM T cells and naïve T cells have distinct TCR repertoires. We compared TCRα sequences and showed that TCR repertoire is distinct between 'VM T-cells' and 'naïve T-cells'. Moreover, T cells with TCRs derived initially from 'VM T-cell clones' differentiated into a VM population and these clones were also detected in naïve population. In contrast, TCRs from 'naïve clones' were almost exclusively detected in naïve T cells.

Additional experiments performed in our laboratory revealed that TCRs enabling the formation of VM T cells are more self-reactive (measured as levels of a self-reactivity marker, CD5) than 'naïve clones'. This is in agreement with the recent observation that $CD5^{hi}$ naïve T cells more frequently differentiate into VM T cells upon an adoptive transfer to lymphoreplete hosts than $CD5^{lo}$ T cells (57). Thus our analysis of TCR repertoire of VM and naïve T cells and retrogenic monoclonal T-cell population showed that VM T-cell formation depends on the level of self-reactivity of a particular T cell. Only highly self-reactive T-cell clones can differentiate into VM $CD8^+$ T cells, whereas less self-reactive T cells remain naïve. These data supported our hypothesis that the formation of VM T cells is a so far unappreciated T-cell fate decision checkpoint, where the intensity of homeostatic TCR signals is the critical decisive factor (Fig. 13) (70).

We also addressed observation made by Renkema et al. (62). They proposed that VM CD8$^+$ T cells are formed from clones using endogenous TCRα and thus TCR specificity plays role in the VM CD8$^+$ T cells formation during ageing. We proposed that T-cell clones using endogenous TCRα formed VM CD8$^+$ T cells because they are more self-reactive than OT-I T cells (data not shown) (62,70).

Results generated during my diploma project were included in our recent publication, in which we clarified the role of TCR specificity and self-reactivity in VM CD8$^+$ T-cells formation (70). We observed that for the formation of VM CD8$^+$ T cells is crucial strength of homeostatic TCRs signals induced by self-antigens.

Due to our findings that TCR repertoire is distinct between VM and naïve T-cell subsets, we wanted to characterize the signaling of particular OVA-reactive TCRs from both naïve and VM subsets. We cloned particular 'VM' and 'naïve clones' into retroviral pMSCV-GFP or pMSCV-LNGFR vectors and transduced them into Jurkat CD8$^+$ OT-I TCRβ T cells and LckKO CD8$^+$ OT-I TCRβ reintroduced with Lck, respectively. We chose the Jurkat cells because they represent a robust system for testing the TCR responsiveness. The main advantage is that Jurkat cell lines are transformed cells which allowed us to repeatedly use a large number of the cells for *in vitro* experiments. Jurkat cell clone with Lck was used because previous experiments performed in our laboratory showed its effective responsiveness to OVA peptide.

Although, we used TCRs that were successfully cloned and sequenced in the first part of the thesis, one 'naïve clone' and one 'VM clone' did not react to OVA at all. Since we saw the same results in the experiment using primary cells, the most possible explanation is that these TCRs had different specificity. For other 6 clones (three 'VM clones', and three 'naïve clones'), we confirmed that they are specific to Kb-OVA.

We expected that the intrinsic response of ‘naïve’ and ‘VM TCRs’ to their cognate antigen would be comparable. However, we observed differences in their responsiveness to OVA which correlated with the level of self-reactivity of particular clones. The most possible explanation of this observation is that TCRs from ‘naïve clones’ might interfere with endogenous TCR of Jurkat cells (e.g., pairing with endogenous TCR chains and our competition for CD3 molecules with the endogenous TCR) which caused the lesser intrinsic response of ‘naïve clones’ to their cognate antigen (OVA peptide).

Collectively, in this part of my thesis, we successfully expressed several functional TCRs from both VM and naïve subsets that were reactive to OVA in two Jurkat cell lines. We performed numerous experiments and observed, that clones with TCR from VM/naïve T cells react to OVA differently. ‘VM clones’ reacted to OVA better than less self-reactive ‘naïve clones’ in both used Jurkat cell lines.

Last but not least, we developed and optimized a qPCR-based method to monitor the behaviour of particular T-cell clones during the course of the immune response. The main reason was that the monitoring *in vivo* is technically demanding, because after activation we can no longer recognize which clones were originally VM and which were naïve.

We designed several functional primers which amplified desired group of clones (i.e., ‘VM clones’ and ‘naïve clones’.) This qPCR-based method will be use for the detection of the relative abundance of clonotypes with low and high level of self-reactivity, respectively, during the onset of immune responses in various organs. As well, we will use this method for the detection of infiltration progeny of VM and naïve T cells in the pancreas during the diabetes in the experimental model of autoimmunity using RIP-OVA mice (75).

However, certain limitation of this method is that it combines detection of ‘naïve’ vs. ‘VM clones’ and high self-reactive clones within naïve subset. Although we saw the VM T-cell clonotype was more enriched during the initial immune response compared to naïve T cells, the reason of this observation remains questionable. One possible explanation is that OVA-reactive VM T cells consisting of ‘VM clones’ expanded more than naïve T cells (enriched for ‘naïve clones’). This is in agreement with the observation made by Lee et al. (69), who observed a stronger initial expansion of adoptively transferred VM OVA-specific T cells than that of naïve OVA-specific T cells upon infection with Lm-OVA. The second explanation of our observation is that the highly self-reactive naïve T cells (VM clones contained within the naïve T-cell pool) expanded more in response to Lm.OVA infection than less self-reactive T cells (naïve clones). This concept is in agreement with the study made by Fulton et al. where they analysed naïve T cells based on their level of self-reactivity. They showed that highly self-reactive naïve T cells consisted of more efficient initial expansion and activation (21).

Due to our technical problems with tetramer staining and low numbers of Vβ5 mice, we performed only one experiment in which we compared immunized (Lm.OVA) and non-immunized Vβ5 mice. In the near future, we aim to repeat this experiment several times and quantify particular clonotypes at different time points. Moreover, we aim to quantify particular clonotypes in different sorted T-cell subsets, and in different organs and study the biology of ‘VM’ and ‘naïve clonotypes’ prior to and during the immune response.

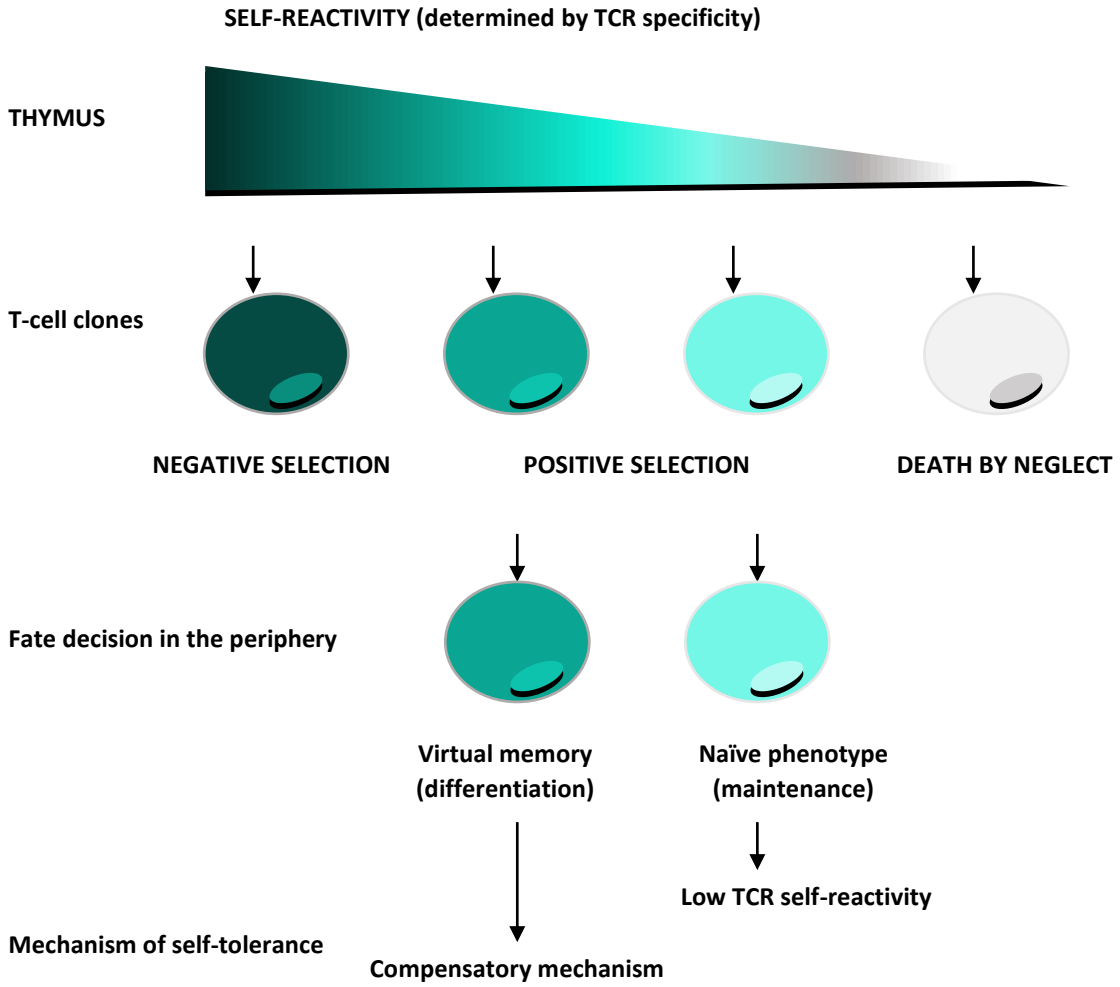

Fig.13: Representation of the role of self-reactivity in major cell fate decisions of conventional $CD8^+$ T cells (70). In lymphoreplete mice, only peripheral $CD8^+$ T cells with relatively high self-reactivity (but below the threshold for negative selection) can differentiate into virtual memory T cells.

8 Summary

The main aim of this thesis was to characterize some features of VM $CD8^+$ T cells and analyze whether they differ in their functions compared to naïve $CD8^+$ T cells.

- We cloned TCRα chains from OVA-reactive naïve and virtual memory T cells from our Vβ5 mouse that had a fixed TCRβ chain. The TCRα sequences were compared to elucidate whether the naïve and virtual memory T-cell clones used different TCRs. We observed that TCR repertoire is distinct between VM and naïve T-cell subsets and that only specific clonotypes have the potential to differentiation into VM T cells.
- We expressed these OVA-reactive TCRs in two Jurkat cell lines and characterized their intrinsic response to Ovalbumin (OVA; SIINFEKL peptide). 6 out of 8 tested TCRs were responsive to Kb-OVA.
- We developed and optimized a qPCR-based method to study the abundance of particular T-cell clonotypes (or groups of clonotypes) during the immune response. We observed that more self-reactive clones were more enriched during initial phase of infection than naïve clones.

9 References

1. Godfrey DI, Kennedy J, Suda T, Zlotnik A. A developmental pathway involving four phenotypically and functionally distinct subsets of CD3-CD4-CD8- triple-negative adult mouse thymocytes defined by CD44 and CD25 expression. J Immunol Baltim Md 1950. 1993 May 15;150(10):4244–52.

2. Laky K, Fowlkes B. Receptor signals and nuclear events in CD4 and CD8 T cell lineage commitment. Curr Opin Immunol. 2005 Apr;17(2):116–21.

3. Sallusto F, Geginat J, Lanzavecchia A. CENTRAL MEMORY AND EFFECTOR MEMORY T CELL SUBSETS : Function, Generation, and Maintenance. Annu Rev Immunol. 2004 Apr;22(1):745–63.

4. Cho BK, Wang C, Sugawa S, Eisen HN, Chen J. Functional differences between memory and naive CD8 T cells. Proc Natl Acad Sci. 1999 Mar 16;96(6):2976–81.

5. Veillette A, Bookman MA, Horak EM, Bolen JB. The CD4 and CD8 T cell surface antigens are associated with the internal membrane tyrosine-protein kinase p56lck. Cell. 1988 Oct 21;55(2):301–8.

6. van Oers NS, Killeen N, Weiss A. ZAP-70 is constitutively associated with tyrosine-phosphorylated TCR zeta in murine thymocytes and lymph node T cells. Immunity. 1994 Nov;1(8):675–85.

7. Balagopalan L, Kortum RL, Coussens NP, Barr VA, Samelson LE. The Linker for Activation of T Cells (LAT) Signaling Hub: From Signaling Complexes to Microclusters. J Biol Chem. 2015 Oct 30;290(44):26422–9.

8. Smith-Garvin JE, Koretzky GA, Jordan MS. T Cell Activation. Annu Rev Immunol. 2009 Apr;27(1):591–619.

9. Cruz-Orcutt N, Vacaflores A, Connolly SF, Bunnell SC, Houtman JCD. Activated PLC-γ1 is catalytically induced at LAT but activated PLC-γ1 is localized at both LAT- and TCR-containing complexes. Cell Signal. 2014 Apr;26(4):797–805.

10. Courtney AH, Lo W-L, Weiss A. TCR Signaling: Mechanisms of Initiation and Propagation. Trends Biochem Sci. 2018 Feb;43(2):108–23.

11. Lewis RS. CALCIUM SIGNALING MECHANISMS IN T LYMPHOCYTES. Annu Rev Immunol. 2001 Apr;19(1):497–521.

12. Takeda S, Rodewald HR, Arakawa H, Bluethmann H, Shimizu T. MHC class II molecules are not required for survival of newly generated CD4+ T cells, but affect their long-term life span. Immunity. 1996 Sep;5(3):217–28.

13. Tanchot C, Lemonnier FA, Pérarnau B, Freitas AA, Rocha B. Differential requirements for survival and proliferation of CD8 naïve or memory T cells. Science. 1997 Jun 27;276(5321):2057–62.

14. Brocker T. Survival of mature CD4 T lymphocytes is dependent on major histocompatibility complex class II-expressing dendritic cells. J Exp Med. 1997 Oct 20;186(8):1223–32.

15. Kirberg J, Berns A, Boehmer H von. Peripheral T Cell Survival Requires Continual Ligation of the T Cell Receptor to Major Histocompatibility Complex–Encoded Molecules. J Exp Med. 1997 Oct 20;186(8):1269–75.

16. Beutner U. TCR-MHC class II interaction is required for peripheral expansion of CD4 cells in a T cell-deficient host. Int Immunol. 1998 Mar 1;10(3):305–10.

17. Müllbacher A. The long-term maintenance of cytotoxic T cell memory does not require persistence of antigen. J Exp Med. 1994 Jan 1;179(1):317–21.

18. Murali-Krishna K. Persistence of Memory CD8 T Cells in MHC Class I-Deficient Mice. Science. 1999 Nov 12;286(5443):1377–81.

19. Swain SL. Class II-Independent Generation of CD4 Memory T Cells from Effectors. Science. 1999 Nov 12;286(5443):1381–3.

20. Štefanová I, Hemmer B, Vergelli M, Martin R, Biddison WE, Germain RN. TCR ligand discrimination is enforced by competing ERK positive and SHP-1 negative feedback pathways. Nat Immunol. 2003 Mar;4(3):248–54.

21. Fulton RB, Hamilton SE, Xing Y, Best JA, Goldrath AW, Hogquist KA, et al. The TCR's sensitivity to self peptide–MHC dictates the ability of naive CD8+ T cells to respond to foreign antigens. Nat Immunol. 2015 Jan;16(1):107–17.

22. Takada K, Jameson SC. Naive T cell homeostasis: from awareness of space to a sense of place. Nat Rev Immunol. 2009 Dec;9(12):823–32.

23. Kamimura D, Atsumi T, Stofkova A, Nishikawa N, Ohki T, Suzuki H, et al. Naïve T Cell Homeostasis Regulated by Stress Responses and TCR Signaling. Front Immunol. 2015 Dec17. Availablefrom:http://journal.frontiersin.org/Article/10.3389/fimmu.2015.00638

24. Azzam HS, Grinberg A, Lui K, Shen H, Shores EW, Love PE. CD5 expression is developmentally regulated by T cell receptor (TCR) signals and TCR avidity. J Exp Med. 1998 Dec 21;188(12):2301–11.

25. Azzam HS, DeJarnette JB, Huang K, Emmons R, Park C-S, Sommers CL, et al. Fine Tuning of TCR Signaling by CD5. J Immunol. 2001 May 1;166(9):5464–72.

26. Hogquist KA, Jameson SC. The self-obsession of T cells: how TCR signaling thresholds affect fate 'decisions' and effector function. Nat Immunol. 2014 Sep;15(9):815–23.

27. Tarakhovsky A, Kanner S, Hombach J, Ledbetter J, Muller W, Killeen N, et al. A role for CD5 in TCR-mediated signal transduction and thymocyte selection. Science. 1995 Jul 28;269(5223):535–7.

28. Dong B, Somani A-K, Love PE, Zheng X, Chen X, Zhang J. CD5-mediated inhibition of TCR signaling proceeds normally in the absence of SHP-1. Int J Mol Med. 2016 Jul;38(1):45–56.

29. Peña-Rossi C, Zuckerman LA, Strong J, Kwan J, Ferris W, Chan S, et al. Negative regulation of CD4 lineage development and responses by CD5. J Immunol Baltim Md 1950. 1999 Dec 15;163(12):6494–501.

30. Mandl JN, Monteiro JP, Vrisekoop N, Germain RN. T cell-positive selection uses self-ligand binding strength to optimize repertoire recognition of foreign antigens. Immunity. 2013 Feb 21;38(2):263–74.

31. Moran AE, Holzapfel KL, Xing Y, Cunningham NR, Maltzman JS, Punt J, et al. T cell receptor signal strength in Treg and iNKT cell development demonstrated by a novel fluorescent reporter mouse. J Exp Med. 2011 Jun 6;208(6):1279–89.

32. Zinzow-Kramer WM, Weiss A, Au-Yeung BB. Adaptation by naïve CD4 $^{+}$ T cells to self-antigen–dependent TCR signaling induces functional heterogeneity and tolerance. Proc Natl Acad Sci. 2019 Jul 8;201904096.

33. Swee LK, Tan ZW, Sanecka A, Yoshida N, Patel H, Grotenbreg G, et al. Peripheral self-reactivity regulates antigen-specific CD8 T-cell responses and cell division under physiological conditions. Open Biol. 2016 Nov;6(11):160293.

34. Kirak O, Frickel E-M, Grotenbreg GM, Suh H, Jaenisch R, Ploegh HL. Transnuclear Mice with Predefined T Cell Receptor Specificities Against Toxoplasma gondii Obtained via SCNT. Science. 2010 Apr 9;328(5975):243–8.

35. Weber KS, Li Q-J, Persaud SP, Campbell JD, Davis MM, Allen PM. Distinct CD4+ helper T cells involved in primary and secondary responses to infection. Proc Natl Acad Sci. 2012 Jun 12;109(24):9511–6.

36. Graw F, Weber KS, Allen PM, Perelson AS. Dynamics of CD4 $^{+}$ T Cell Responses against *Listeria monocytogenes*. J Immunol. 2012 Dec 1;189(11):5250–6.

37. Persaud SP, Parker CR, Lo W-L, Weber KS, Allen PM. Intrinsic CD4+ T cell sensitivity and response to a pathogen are set and sustained by avidity for thymic and peripheral complexes of self peptide and MHC. Nat Immunol. 2014 Mar;15(3):266–74.

38. Polic B, Kunkel D, Scheffold A, Rajewsky K. How T cells deal with induced TCR ablation. Proc Natl Acad Sci. 2001 Jul 17;98(15):8744–9.

39. Wiehagen KR, Corbo E, Schmidt M, Shin H, Wherry EJ, Maltzman JS. Loss of tonic T-cell receptor signals alters the generation but not the persistence of CD8+ memory T cells. Blood. 2010 Dec 16;116(25):5560–70.

40. Myers DR, Lau T, Markegard E, Lim HW, Kasler H, Zhu M, et al. Tonic LAT-HDAC7 Signals Sustain Nur77 and Irf4 Expression to Tune Naive CD4 T Cells. Cell Rep. 2017 May;19(8):1558–71.

41. Levine AG, Arvey A, Jin W, Rudensky AY. Continuous requirement for the TCR in regulatory T cell function. Nat Immunol. 2014 Nov;15(11):1070–8.

42. Corbo-Rodgers E, Wiehagen KR, Staub ES, Maltzman JS. Homeostatic Division Is Not Necessary for Antigen-Specific CD4 $^{+}$ Memory T Cell Persistence. J Immunol. 2012 Oct 1;189(7):3378–85.

43. Mosmann TR, Cherwinski H, Bond MW, Giedlin MA, Coffman RL. Two types of murine helper T cell clone. I. Definition according to profiles of lymphokine activities and secreted proteins. J Immunol Baltim Md 1950. 1986 Apr 1;136(7):2348–57.

44. Park H, Li Z, Yang XO, Chang SH, Nurieva R, Wang Y-H, et al. A distinct lineage of CD4 T cells regulates tissue inflammation by producing interleukin 17. Nat Immunol. 2005 Nov;6(11):1133–41.

45. Zhu J, Yamane H, Paul WE. Differentiation of Effector CD4 T Cell Populations. Annu Rev Immunol. 2010 Mar;28(1):445–89.

46. Dequiedt F, Kasler H, Fischle W, Kiermer V, Weinstein M, Herndier BG, et al. HDAC7, a thymus-specific class II histone deacetylase, regulates Nur77 transcription and TCR-mediated apoptosis. Immunity. 2003 May;18(5):687–98.

47. Markegard E, Trager E, Yang CO, Zhang W, Weiss A, Roose JP. Basal LAT-diacylglycerol-RasGRP1 signals in T cells maintain TCRα gene expression. PloS One. 2011;6(9):e25540.

48. Bhandoola A, Tai X, Eckhaus M, Auchincloss H, Mason K, Rubin SA, et al. Peripheral Expression of Self-MHC-II Influences the Reactivity and Self-Tolerance of Mature CD4+ T Cells. Immunity. 2002 Oct;17(4):425–36.

49. Smith K, Seddon B, Purbhoo MA, Zamoyska R, Fisher AG, Merkenschlager M. Sensory Adaptation in Naive Peripheral CD4 T Cells. J Exp Med. 2001 Nov 5;194(9):1253–62.

50. Stefanová I, Dorfman JR, Germain RN. Self-recognition promotes the foreign antigen sensitivity of naive T lymphocytes. Nature. 2002 Nov;420(6914):429–34.

51. Vahl JC, Drees C, Heger K, Heink S, Fischer JC, Nedjic J, et al. Continuous T Cell Receptor Signals Maintain a Functional Regulatory T Cell Pool. Immunity. 2014 Nov;41(5):722–36.

52. White JT, Cross EW, Kedl RM. Antigen-inexperienced memory CD8+ T cells: where they come from and why we need them. Nat Rev Immunol. 2017 May 8;17(6):391–400.

53. Broussard C, Fleischecker C, Horai R, Chetana M, Venegas AM, Sharp LL, et al. Altered Development of CD8+ T Cell Lineages in Mice Deficient for the Tec Kinases Itk and Rlk. Immunity. 2006 Jul;25(1):93–104.

54. Horai R, Mueller KL, Handon RA, Cannons JL, Anderson SM, Kirby MR, et al. Requirements for Selection of Conventional and Innate T Lymphocyte Lineages. Immunity. 2007 Nov;27(5):775–85.

55. Cho BK, Rao VP, Ge Q, Eisen HN, Chen J. Homeostasis-stimulated proliferation drives naive T cells to differentiate directly into memory T cells. J Exp Med. 2000 Aug 21;192(4):549–56.

56. Haluszczak C, Akue AD, Hamilton SE, Johnson LDS, Pujanauski L, Teodorovic L, et al. The antigen-specific CD8 $^{+}$ T cell repertoire in unimmunized mice includes memory phenotype cells bearing markers of homeostatic expansion. J Exp Med. 2009 Feb 16;206(2):435–48.

57. White JT, Cross EW, Burchill MA, Danhorn T, McCarter MD, Rosen HR, et al. Virtual memory T cells develop and mediate bystander protective immunity in an IL-15-dependent manner. Nat Commun. 2016 Apr 21;7:11291.

58. Lee YJ, Holzapfel KL, Zhu J, Jameson SC, Hogquist KA. Steady-state production of IL-4 modulates immunity in mouse strains and is determined by lineage diversity of iNKT cells. Nat Immunol. 2013 Nov;14(11):1146–54.

59. Tan JT, Dudl E, LeRoy E, Murray R, Sprent J, Weinberg KI, et al. IL-7 is critical for homeostatic proliferation and survival of naive T cells. Proc Natl Acad Sci. 2001 Jul 17;98(15):8732–7.

60. Sosinowski T, White JT, Cross EW, Haluszczak C, Marrack P, Gapin L, et al. CD8 + Dendritic Cell Trans Presentation of IL-15 to Naive CD8+ T Cells Produces Antigen-Inexperienced T Cells in the Periphery with Memory Phenotype and Function. J Immunol. 2013 Mar 1;190(5):1936–47.

61. Tripathi P, Morris SC, Perkins C, Sholl A, Finkelman FD, Hildeman DA. IL-4 and IL-15 promotion of virtual memory CD8 $^{+}$ T cells is determined by genetic background. Eur J Immunol. 2016 Oct;46(10):2333–9.

62. Renkema KR, Li G, Wu A, Smithey MJ, Nikolich-Zugich J. Two Separate Defects Affecting True Naive or Virtual Memory T Cell Precursors Combine To Reduce Naive T Cell Responses with Aging. J Immunol. 2014 Jan 1;192(1):151–9.

63. Kurzweil V, LaRoche A, Oliver PM. Increased Peripheral IL-4 Leads to an Expanded Virtual Memory CD8+ Population. J Immunol. 2014 Jun 15;192(12):5643–51.

64. Prince AL, Kraus Z, Carty SA, Ng C, Yin CC, Jordan MS, et al. Development of Innate CD4 $^{+}$ and CD8 $^{+}$ T Cells in Itk-Deficient Mice Is Regulated by Distinct Pathways. J Immunol. 2014 Jul 15;193(2):688–99.

65. Huang W, Huang F, Kannan AK, Hu J, August A. ITK tunes IL-4-induced development of innate memory CD8 $^{+}$ T cells in a γδ T and invariant NKT cell-independent manner. J Leukoc Biol. 2014 Jul;96(1):55–63.

66. Pribikova M, Moudra A, Stepanek O. Opinion: Virtual memory CD8 T cells and lymphopenia-induced memory CD8 T cells represent a single subset: Homeostatic memory T cells. Immunol Lett. 2018 Nov;203:57–61.

67. Akue AD, Lee J-Y, Jameson SC. Derivation and maintenance of virtual memory CD8 T cells. J Immunol Baltim Md 1950. 2012 Mar 15;188(6):2516–23.

68. Chiu B-C, Martin BE, Stolberg VR, Chensue SW. Cutting Edge: Central Memory CD8 T Cells in Aged Mice Are Virtual Memory Cells. J Immunol. 2013 Dec 15;191(12):5793–6.

69. Lee J-Y, Hamilton SE, Akue AD, Hogquist KA, Jameson SC. Virtual memory CD8 T cells display unique functional properties. Proc Natl Acad Sci. 2013 Aug 13;110(33):13498–503.

70. Drobek A, Moudra A, Mueller D, Huranova M, Horkova V, Pribikova M, et al. Strong homeostatic TCR signals induce formation of self-tolerant virtual memory CD8 T cells. EMBO J. 2018 Jul 13;37(14):e98518.

71. Rolot M, Dougall AM, Chetty A, Javaux J, Chen T, Xiao X, et al. Helminth-induced IL-4 expands bystander memory CD8+ T cells for early control of viral infection. Nat Commun 2018 Dec. Available from: http://www.nature.com/articles/s41467-018-06978-5

72. Lin JS, Mohrs K, Szaba FM, Kummer LW, Leadbetter EA, Mohrs M. Virtual memory CD8 T cells expanded by helminth infection confer broad protection against bacterial infection. Mucosal Immunol. 2019 Jan;12(1):258–64.

73. Sprent J, Surh CD. Normal T cell homeostasis: the conversion of naive cells into memory-phenotype cells. Nat Immunol. 2011 Jun;12(6):478–84.

74. Fink PJ, Swan K, Turk G, Moore MW, Carbone FR. Both intrathymic and peripheral selection modulate the differential expression of V beta 5 among CD4+ and CD8+ T cells. J Exp Med. 1992 Dec 1;176(6):1733–8.

75. Kurts C, Miller JF, Subramaniam RM, Carbone FR, Heath WR. Major histocompatibility complex class I-restricted cross-presentation is biased towards high dose antigens and those released during cellular destruction. J Exp Med. 1998 Jul 20;188(2):409–14.